FEASIBILITY STUDY OF A SYNTHESIS PROCEDURE FOR ARRAY FEEDS TO IMPROVE RADIATION PERFORMANCE OF LARGE DISTORTED REFLECTOR ANTENNAS

Grant No. NAG-1-859

SEMIANNUAL STATUS REPORT

by

W.L. Stutzman
K. Takamizawa
P. Werntz
J. LaPean
R. Barts

Virginia Polytechnic Institute and State University
Bradley Department of Electrical Engineering
Blacksburg, VA 24061-0111

February 1991

TABLE OF CONTENTS

1. INTRODUCTION

Virginia Tech is involved in a number of activities with NASA Langley related to large aperture radiometric antenna systems. These efforts are summarized in Table 1-1. This semi-annual report is directed toward the grant first listed in Table 1-1; however, the efforts are so closely related that activities on those are reported here as well.

The theoretical design procedures of array feeds to compensate for distortions on the surface of reflectors was completed and reported on in the previous semi-annual report. Since then a manuscript for a major journal article was prepared and submitted with an approval copy sent to LaRC. Further documentation of that effort continues.

Table 1-2 lists the major reflector antenna research areas together with the students performing the work. Table 1-3 details specific near-term tasks in each of the intensive work areas.

This report is organized into sections reflective of the work areas as listed in Table 1-2.

Table 1-1

REFLECTOR ANTENNA RESEARCH AT VIRGINIA TECH

1. "Feasibility Study of a Synthesis Procedure for Array Feeds to Improve Radiation Performance of Large Distorted Reflector Antennas"

   GAs: Ko Takamizawa, Jim LaPean
   Project: NASA Grant NAG-1-859; VT 4-26132
   Term: 02/25/88 - 12/31/91

2. "Definition of Large Deployable Space Antenna Structure Concept"

   GA: Paul Werntz
   Project: NASA Contract NAS-1-18471-Task 18; VT 4-26182
   Term: 02/15/89 - 04/14/92

3. "Design of Array Feeds for Large Reflector Antennas"

   GA: Mike Barts
   Project: NASA Graduate Student Researchers Program; NGT-50413; VT 4-26204
   Term: 08/16/89 - 08/15/91

Table 1-2

REFLECTOR ANTENNA RESEARCH ACTIVITIES AT VIRGINIA TECH

I. Technology Development - Takamizawa
   1. Operation and testing of full commercial reflector code (GRASP7) - Takamizawa
   2. Multiple reflector cylindrical antenna code (MRAPCA) - Takamizawa
   3. Documentation of analysis techniques for reflector computations - Takamizawa
   4. Development of synthesis codes (RAPSYN) for concept antennas - Werntz, Takamizawa, Shen

II. Wide Scanning Antenna Systems
   1. Documentation of wide scanning antenna principles - Werntz
   2. Dual Parabolic Reflector - Takamizawa
   3. Spherical Reflector Family - Werntz
   4. Cylindrical Reflector Family
   5. Toroidal reflector family
   6. Hybrid concepts

III. LDA Designs - Werntz
   1. Evaluation of Foldes Type 2 variations - Werntz
   2. Detailed analysis of Foldes Type 6 designs - LaPean

IV. Arrays for Large Radiometric Antennas - Barts
   1. Beam efficiency studies
   2. Analysis techniques in lossy radiometric systems using arrays.
   3. Feed array architectures for radiometers
   4. Feed component technology readiness evaluation
   5. Calibration issues

V. Electronic Compensation for Surface Distortion Effects
   W. Smith (now at U. of Kentucky)

Table 1-3

NEAR TERM REFLECTOR ANTENNA RESEARCH TASKS

I. **Technology development** - Takamizawa
   1.1 Coordinate in the installation of the GRASP7 code at Langley
   1.2 Complete graphic support of GRASP7

II. **Wide Scanning Antenna Systems**
   2.1 Documentation of wide Scanning system - Werntz
   2.2 Dual parabolic reflectors - Takamizawa
      a. Document the technology
      b. Relate to recent hardware (Comsat, Harris)
      c. Computer runs to evaluate promise of dual parabolas
   2.3 Spherical reflector - Werntz

III. **LSA Designs** - Werntz
   3.1 Offset Parabola (Foldes Type 2) - Werntz
      a. Design correcting (rotating, active shaping) tertiary subreflector configuration in 2D: Complete
      b. Evaluate with parabolic main reflector, elliptic first subreflector, and tertiary subreflector.
         - Rotating tertiary
         - Moving and rotating tertiary
         - Optimize geometry for Gregorian case (low F, location of feed)
         - Reshape sub after shaping tertiary
         - Above first in 2D, then 3D
      c. M.C. Bailey design the feed array feed.
      d. Investigate feed arrays to obviate shaping tertiary
   3.2 Offset Parabola (Foldes Type 6) - LaPean
      a. Design correcting (active shaping) subreflector configuration in 2D: complete
      b. Evaluate with an optimum motion (statically shaped) subreflector configuration in 2D
         - Rotate subreflector about feed location
         - Rotate subreflector about scanned virtual focus
         - Other subreflector motions
      c. Design correcting (active shaping) subreflector configuration in 3D
      d. Evaluate with an optimum motion (statically shaped) subreflector configuration in 3D
      e. Evaluate with an optimum motion (statically shaped) subreflector and compensating array feed in 3D. (Technical support from M.C. Bailey)

IV. **Radiometric arrays** - Barts
   4.1 Complete, document, and distribute analysis
   4.2 Calibration methods
   4.3 Common aperture feed arrays

2. TECHNOLOGY DEVELOPMENT

This area supports the investigation areas, primarily in the form of computer code development. Here we report on the main codes in active use.

2.1 GRASP7

General Reflector Antenna Systems Program version 7 (GRASP7) is a program to compute radiation patterns of three dimensional single or dual reflector antennas. Developed by TICRA in Denmark, the program uses a combination of the physical optics (PO) and the geometrical theory of diffraction (GTD) to compute the patterns. A summary of GRASP7 capabilities are shown in Table 2.1-1. The program has been installed and tested on the IBM 3090 computer at Virginia Tech.

Some modifications have been made to GRASP7 to allow analysis of reflector concepts studied at Virginia tech. Non uniformly distributed points to numerically define reflector surface types have been added to both main reflector and subreflector. This reflector type was implemented because the synthesis program TRTDS, which is described in Section 2.3 generates the surface data in uneven distribution. The subroutine uses a modified IMSL surface fit routine IBIRAN which locally fits a fifth order polynomial in each dimension to a given set of surface data. The routine has been tested and verified for the PO analysis which requires only the interpolated surface values and their first partial derivatives. However, the routine does not produce satisfactory results for the GTD analysis which requires the second partial derivatives.

The second addition to GRASP7 was the $\cos^q\theta$ feed element type. The subroutine generates a feed pattern with $\cos^q\theta$ power profile which can be either linearly or circularly polarized. The routine has been verified with results generated by a single reflector antenna analysis program RAP written at Virginia Tech.

Two programs are being developed to support GRASP7: GRASPIN, a preprocessor program, and GRASPOUT, post processor program. GRASPIN is a program which helps the user generate and to edit input files required for GRASP7. GRASPOUT is a program which extracts the calculated results from GRASP7 output files and then creates displays on a CRT or prints to a HP Laser Jet printer. It has the capability to generate feed pattern cuts, secondary pattern cuts, and contour plots. Examples of screen dumps to the laser printer are shown in Figs 2.1-1 and 2.1-2. GRASPOUT can also generate ASCII format data files of the calculated results which can be plotted by a commercially available graphing program; we use AXUM. Both GRASPIN and GRASPOUT are written for IBM PC and compatibles.

Table 2.1-1

Summary of General Reflector Antenna Systems Program (GRASP7)

I. Single or dual reflector antennas with following geometries

A. Reflector surface shapes
(Unless otherwise stated, applies to both main and sub reflector)
a) Parabolic (main reflector)
b) Ellipsoid (sub reflector)
c) Hyperboloid (sub reflector)
d) Surface defined by second order polynomials
e) Arbitrary via tabulated uniformly distributed data points
f) Rotational symmetric tabulated data points
g) Unfurlable rib antenna (main reflector)
h) Unfurlable truss antenna (main reflector)
i) User defined in code

B. Reflector rim shapes
a) Circular
b) Elliptical
c) Superelliptical
d) Tabulated
e) Circular cone for ellipsoid or hyperboloid subreflector
f) User defined in code

C. Reflector surface distortion (main reflector)
a) Tabulated
b) Random (zero mean uniform distribution between peak values)
c) Zernike modes

D. Reflector surface types
a) Perfect conductor
b) Mesh

II. Multiple feeds with following antenna element types

a) $A(\theta) = K \left[\frac{1 \pm \cos \theta}{2} \right]^n$

b) $A(\theta) = K\ 10\ (\theta/\theta_o)^2$

c) Tabulated input data
d) Pyramidal horn
e) Conical horn
f) Rectangular waveguide

g) Circular waveguide
h) Hexagonal waveguide
i) Circular microstrip patch radiator
j) Axial-mode monofilar helix
k) Spiral antenna
l) Spherical wave expansion coefficients
m) Gaussian beam
n) Array of up to 4 half wave dipoles
o) User defined in code

III. Analysis techniques available
a) Physical optics (P.O.)
b) Geometrical theory of diffraction (GTD)

IV. Features permitting analysis of multiple reflectors

V. Modifications made at Virginia Tech
a) Reflector surface fit for non-uniformly distributed data points.
b) cos q θ feed element
- Linear vertical and horizontal polarizations
- Left hand and right hand circular polarizations

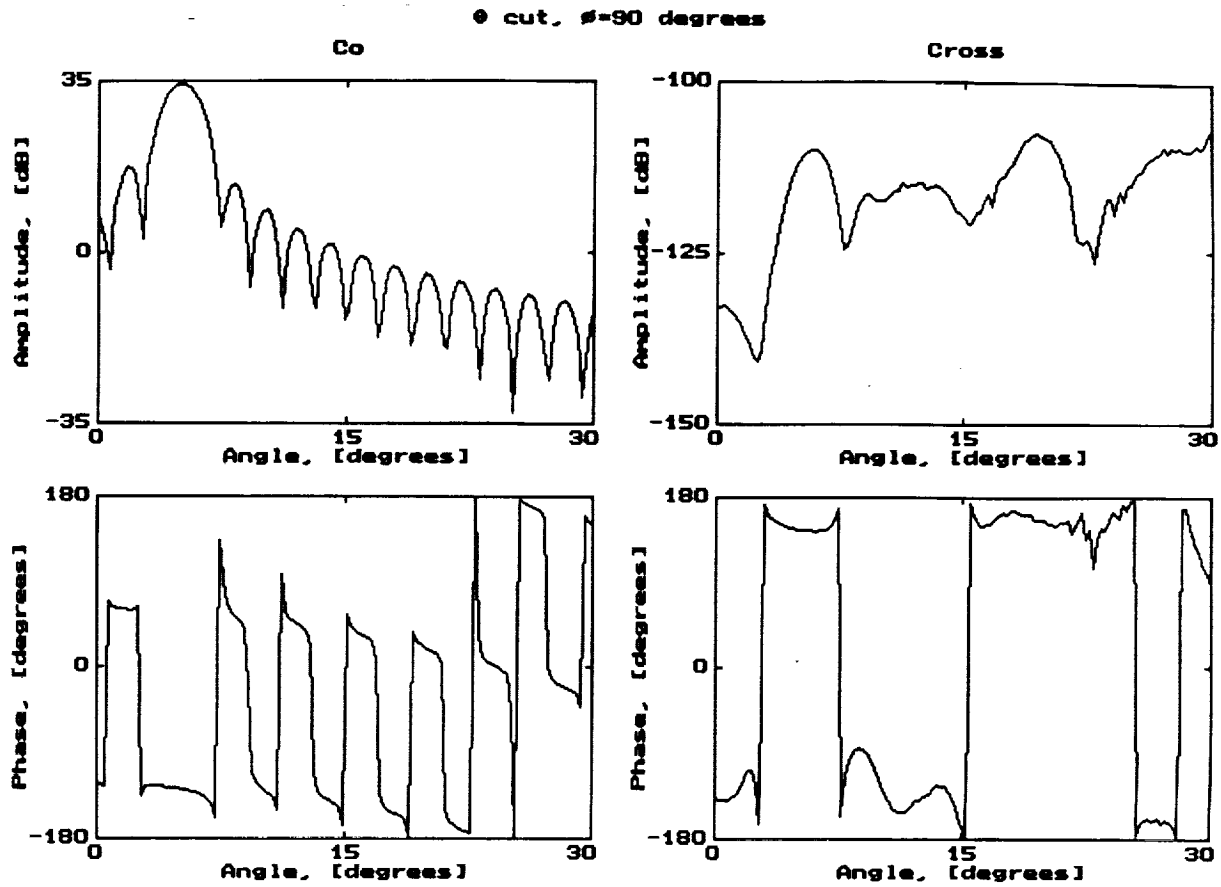

Figure 2.1-1 Secondary pattern cuts generated by GRASPOUT.

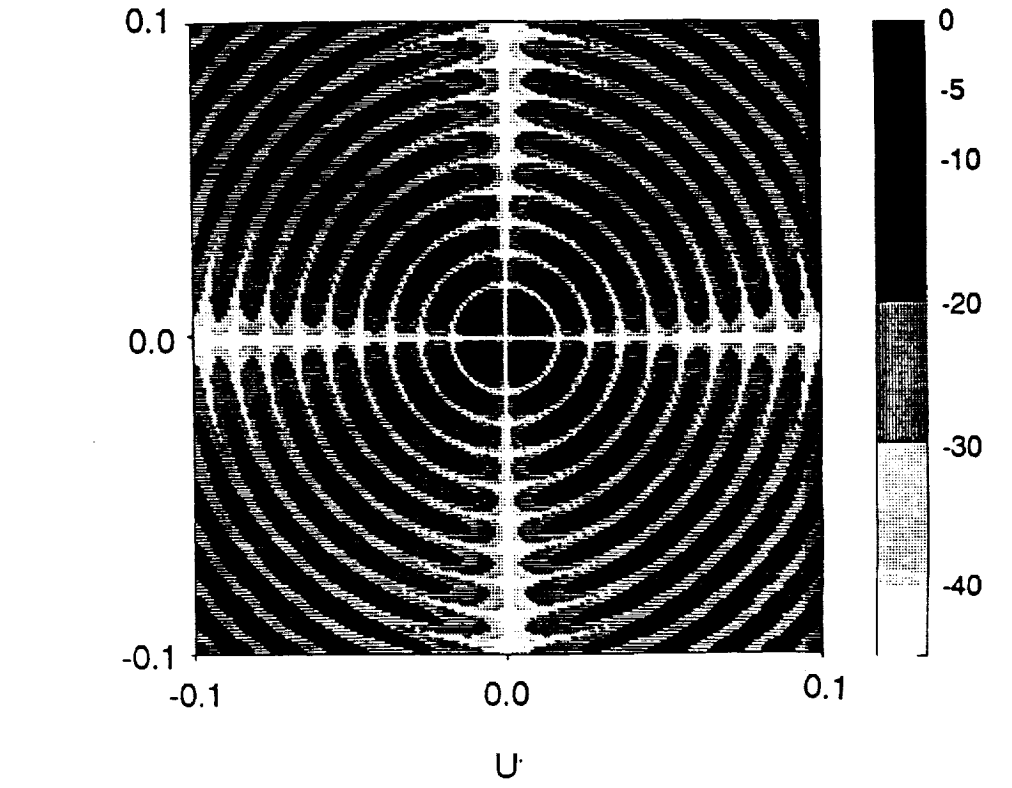

Figure 2.1-2 A contour plot of secondary fields.

Since GRASP7 has been installed at Virginia tech, two updates have been supplied by TICRA. The updated GRASP7 with Virginia Tech modifications (version 7.7, VT version 1.5) has been supplied to NASA LaRC.

2.2 Multiple Reflector Analysis Program for Cylindrical Antennas (MRAPCA)

The program MRAPCA (Multiple Reflector Analysis Program for Cylindrical Antennas) was written to facilitate the two-dimensional radiation pattern analysis of multiple cylindrical reflectors. The patterns are computed using near-field physical optics/aperture integration (NF-PO/AI) and/or far-field physical optics/aperture integration (FF-PO/AI) depending on the desired output. A summary of MRAPCA capabilities are shown in Table 2.2-1. MRAPCA is used extensively to test wide scan concepts and their performances. It has been used to investigate both Foldes Type 2 and Type 6 concepts, as well as spherical and imaging systems.

Several additions and improvements were implemented to MRAPCA in this reporting period. A plane wave feed incident from an arbitrary angle was implemented. The plane wave can be used to illuminate the main subreflector. When a plane wave illuminates the main reflector, the focal plane region field distribution is calculated. On the other hand, a plane wave used to illuminate subreflector aids in the investigation of ideal performance of the multiple reflector imaging system which will be discussed in Section 3.3.

In addition to the far-field pattern, MRAPCA can now calculate aperture field pattern of the main reflector using NF-PO. The output from the program can then be used in conjunction with the array feed optimization program written by M.C. Bailey to design an array feed for a particular reflector system geometry. It was also pointed out by Peter Foldes that the performance of a particular reflector system can be estimated by the aperture field rather than the secondary pattern of the reflector. This eliminates the step of far field evaluation.

Table 2.2-1

Summary of Multiple Reflector Analysis Program for Cylindrical Antenna (MRAPCA)

Reflector Geometry - Any combination of the following surfaces.

- Analytical Surfaces
  - Parabola
  - Hyperbola
  - Ellipse
  - Spherical
  - General second order
- Numerically Defined Surfaces
  - Natural cubic spline

Pattern Analysis Techniques - Combination of the following techniques depending on the desired output pattern.

- Near-field Physical Optics/Aperture Integration (NF-PO/AI)
- Far-field Physical Optics/Aperture Integration (FF-PO/AI)

Incident Fields

- Array of $\cos^{q}\theta$ elements - arbitrary amplitude, phase, q, and pointing angle for each element.
- Plane wave incident from angle θ_o - used for the focal plane field analysis.

Computed Output Fields

- Far-field of main reflector.
- Amplitude and phase of aperture field of the main reflector using near-field physical optics.
- Focal plane region pattern - planar cuts or contour.

2.3 Documentation of Analysis Techniques

A Literature survey of the reflector antenna radiation patten analysis techniques was conducted. The outline of a white paper which is currently being written is shown in Table 2.3-1.

2.4 Tri-Reflector Two Dimensional Synthesis Code (TRTDS)

This geometrical optics code is used to synthesize cylindrical three reflector systems such as the Foldes Type 2 and Gregorian Type 2 antennas. It is not limited to these two configurations, however, and may be used to design a correcting tertiary reflector for any reasonable main reflector profile, subreflector profile and feed location.

In order to use the code, one must have analytic expressions for the main reflector, subreflector and both of there surface normals in the two dimensional xz-coordinate system. Given the reflector configuration one then must specify the focal point location, the aperture plane location, the total path length from the feed to the aperture plane and the desired scan direction. Given these data, TRTDS produces a tertiary reflector profile which corrects for aperture phase errors in the given scan direction. This is accomplished by finding ray paths, arising from equally spaced rays incident on the main reflector from the given scan angle and reflected off of the subreflectors subject to Snell's law and the main reflector and subreflector. Next, given the feed location, the intersection points of the rays emanating from the feed and the rays reflected off of the subreflector are found such that the length of all rays from the feed to the defined aperture plane are equal to a specified total path length. The resulting intersection points define the profile of the tertiary reflector.

Geometrical optics synthesis is expected to be reasonably accurate for cases where the reflectors are much larger than a wavelength. For this case, TRTDS code has been verified by the two dimensional physical optics routine MRAPCA (see Section 2.2). It should be noted that TRTDS can be easily extended to allow for measured main reflector and subreflector data by using a numerical interpolatory routine, such as cubic splines, to obtain the necessary reflector surface and normal information between measured points. Currently, this code is being extended for the design of three dimensional reflector systems using an algorithm which has already been applied to three dimensional two reflector systems.

Table 2.3-1

Outline of "Reflector Antenna Analysis Techniques"

1. Introduction

2. First Order analysis of Reflector Radiation Pattern
   - 2.1 Geometrical Optics/Aperture Integration (GO/AI)
   - 2.2 Physical Optics/Surface Integration (PO/SI)
   - 2.3 Comparison of GO/AI and PO/SI
   - 2.4 Evaluation of Radiation Integral

3. Reflector Diffraction Analysis
   - 3.1 Geometrical Theory of Diffraction (GTD) and Uniform Geometrical Theory of Diffraction (UTD)
   - 3.2 Uniform Asymptotic Theory (UAT)
   - 3.3 Asymptotic Transition Region Theory (TRT) and Kinematic and Dynamic Ray Tracing
   - 3.4 Edge current Method (ECM)
   - 3.5 Physical Theory of Diffraction (PTD) and Incremental Diffraction Coefficients

4. Focal Plane Field Analysis

5. Application of Reflector Analysis Techniques in Multiple Reflector Antennas

6. Conclusions

2.5 A Geometrical Optics Synthesis Technique

Our reflector antenna research group includes a Ph.D. student in physics, Bing Shen. Although not supported through LaRC, Bing is a major contributor to our program.

A ray tracing based code "SORT" for scan reflector system synthesis was written based on optimization principles. A range of positions in the focal region that yields minimum phase error effects over the main beam scan range is determined. Several feed locations, and their corresponding final output beam directions are evaluated. Minimizing the optical path length deviation from each of those feed points to its corresponding aperture plane (perpendicular to the output direction) will give a near perfect focal plane. The design goal is to maintain the residue path length deviation after optimization is much less than a wavelength.

The essential features of that code follows:

1. A new ray tracing technique is used which allows solution for a ray for both a specified aperture plane point and feed point. In contrast, Snell's law based ray tracing methods, which traces a ray under given input ray direction without knowing where it eventually leaves the reflector optical system. Our method also has global quadratic convergence property yielding fast computation.

2. Cubic spline interpolation of reflector surface is used, which allows the surface shape description with a small number of parameters. The surface is assumed to be the natural cubic spline interpolation through a few evenly spaced data points. Changing those data points will change the shape.

3. For a given feed point and its aperture plane, a number of points in the aperture plane is sampled and for each of them, a ray is joined between it and the feed point. Once the ray is solved, we can calculate its path length. For all the sampled rays the path length deviation is calculated. A number of feed points are sampled. The sum of their resulting deviations is the total deviation of the reflector optical system. The simplex method for multidimensional optimization is used to minimize the total deviation by changing spline interpolation data points for each reflector.

   The success of this method depends on the initial guess of the reflector system. When implementing this method, we use the deviation of the tangent of the output ray directions to the desired output direction rather than the (equivalent) path length deviation method. This saves computing time and is less sensitive to round off error. In two-reflector and

two-sampled-feed-point case, or tri-reflector and three-sampled-feed-point case, the deviation can be minimized to virtually zero. These bifocal or trifocal cases. We have obtained results for the bifocal system.

2.6 A Physical Optics Synthesis Technique

The geometrical optics (GO) is, by far, the most widely accepted synthesis technique used for the design of reflector antennas. GO is a high frequency approximation which employs rays to describe the fields incident from the source and the fields which are reflected and refracted at an interface between two different media. In the GO synthesis, the geometry of some or all of the reflectors and/or location and radiation patterns of the feed elements are determined by solving equations based on the rays from the feed to the aperture plane of the main reflector.

The GO based techniques have been shown to work well for a simple reflector synthesis where the design specifications are in the co-polar pattern near main beam region or in the main reflector aperture field. When other parameters such as the cross-polarization components, the sidelobe envelopes and the null positions are specified, the GO based techniques usually require "fine tuning" of the reflector geometry by repeated application of post design radiation pattern analysis using physical optics and edge diffraction techniques. This step is necessary since GO analysis cannot accurately predict the sidelobe levels and the cross-polar patterns [Hombuck]. Thus, GO-based synthesis may not be adequate for the design of reflectors for the LSA project where the design requirements are stringent.

An alternative method to synthesize reflector antennas is to use physical optics (PO). The technique permits direct use of specifications discussed above within the synthesis procedure. A simple way to implement the PO synthesis is to define the reflector surface by a series. Then, the radiation patterns of subreflectors in the multi-reflector system can be calculated using PO/AI. An error function can be defined in terms of desired pattern and the calculated pattern. The error function can be also derived in terms of aperture fields or focal plane fields. Then, the error function can be minimized using an ordinary optimization routine to determine the reflector geometry. This technique can be also extended for design of wide scan systems.

In the initial phase of this study, a synthesis technique will be developed for the geometries in two dimensions. The computer program MRAPCA described in Section 2.2 will be modified to create the synthesis code. Koichiro Takamizawa will write his Ph.D. dissertation on the PO synthesis technique.

3. CONCEPTS IN WIDE SCANNING ANTENNA SYSTEMS

Many concepts have been proposed and evaluated to various depths during the course of these efforts. Here we report on the ones that have received the most attention during the reporting period.

3.1 Documentation of Beam Scanning Reflector Systems

A literature survey of beam scanning techniques for reflector antennas was conducted. The outline of a white paper based on these techniques is given in Table 3.1-1.

Table 3.1-1

Outline of White Paper on Beam Scanning Reflector Systems

1. Introduction
   - 1.1 Scalar Diffraction Theory
   - 1.2 Properties of Focusing Aperture Antennas
2. Focal Region of Parabolic Reflectors
   - 2.1 Displaced Feed Scanning
   - 2.2 Butler Matrix Array Feed
   - 2.3 Dual parabolic Array fed Reflector Properties
3. Focal Region of Spherical Reflectors
   - 3.1 Single Reflector Correction
   - 3.2 Multiple Reflector Correction
4. Torus Reflector
5. Array Fed Cylindrical Reflector
6. Extended Focal Region Reflectors
   - 6.1 Bifocal Dual Reflector
   - 6.2 Optimized Multiple Reflector Systems
7. Foldes Type 6 Reflector
8. Type 2 Reflector Antenna Concepts
9. Conclusions

3.2 The Type 2 Reflector Antenna Concepts

The original Type 2 reflector concept is a tri-reflector with an elliptic subreflector in a Cassegrain configuration, and a shaped tertiary reflector. This is the Foldes Type 2 antenna concept. The purpose behind this configuration is to allow for scanning with a minimum of reflector and feed motion without significant loss in gain during scan. The elliptic subreflector has one focus at the center of the main reflector and the other focus at the center of the tertiary reflector. This creates a "conjugate" relation between the two points. Ideally, any ray incident on the center of the main reflector, regardless of incidence angle, will be reflected to the conjugate point at the center of the tertiary reflector. If every point on the main reflector had a conjugate point on the tertiary, then undergraded scan is possible without movement of the tertiary. This is not true for rays striking the main reflector at points either above or below the center point. It is possible to scan the system by a simple rotation of the tertiary reflector about its center point. When scanning; however, only the central ray, which passes through the two conjugate points, experiences no change in path length from the feed to the surface of the main reflector. This means that if scanning is attempted by rotating a tertiary reflector of fixed shape, some aperture phase error will be incurred at all scan angles except for the direction for which the tertiary reflector was designed. Two methods to correct for the aperture phase errors are to either allow for an actively shaped tertiary reflector or to use a (probably small) phased array feed. Other possible ways to partially correct for scan induced phase errors include allowing for a slight translation movement of the tertiary and/or feed element.

The original Foldes Type 2 reflector antenna is shown in Fig. 3.2-1. This reflector system was generated using TRTDS (see Section 2.4) and has a different shape and size correcting tertiary reflector for each scan direction. The dimensions of the reflector antenna were chosen to correspond closely to the dimensions given in a report authored by P. Foldes and dated May 3, 1989. The main reflector diameter is 28 m and the focal length of the main reflector is 55.9 m (F/D = 2). The configuration shown in Fig. 3.2-1 is designed to scan ±2.5°. Under this condition the subreflector diameter is 10.5 m and the tertiary diameter varies from roughly 2.5 m to 6.7 m, the smallest tertiary size corresponding to the -2.5° scan direction and the largest tertiary size corresponding to the +2.5° scan direction. A detailed diagram of tertiary motion is shown in Fig. 3.2-2. Patterns were calculated for this cylindrical configuration at 10 GHz (corresponding to a main reflector diameter of 933 λ) using MRAPCA (see Section 2.2). For all scan angles, a correcting tertiary was used and illuminated with a $\cos^q(\theta)$ feed pattern with q selected to give a -10 dB tertiary edge illumination. The patterns for +2.5°, 0° and -2.5° scan

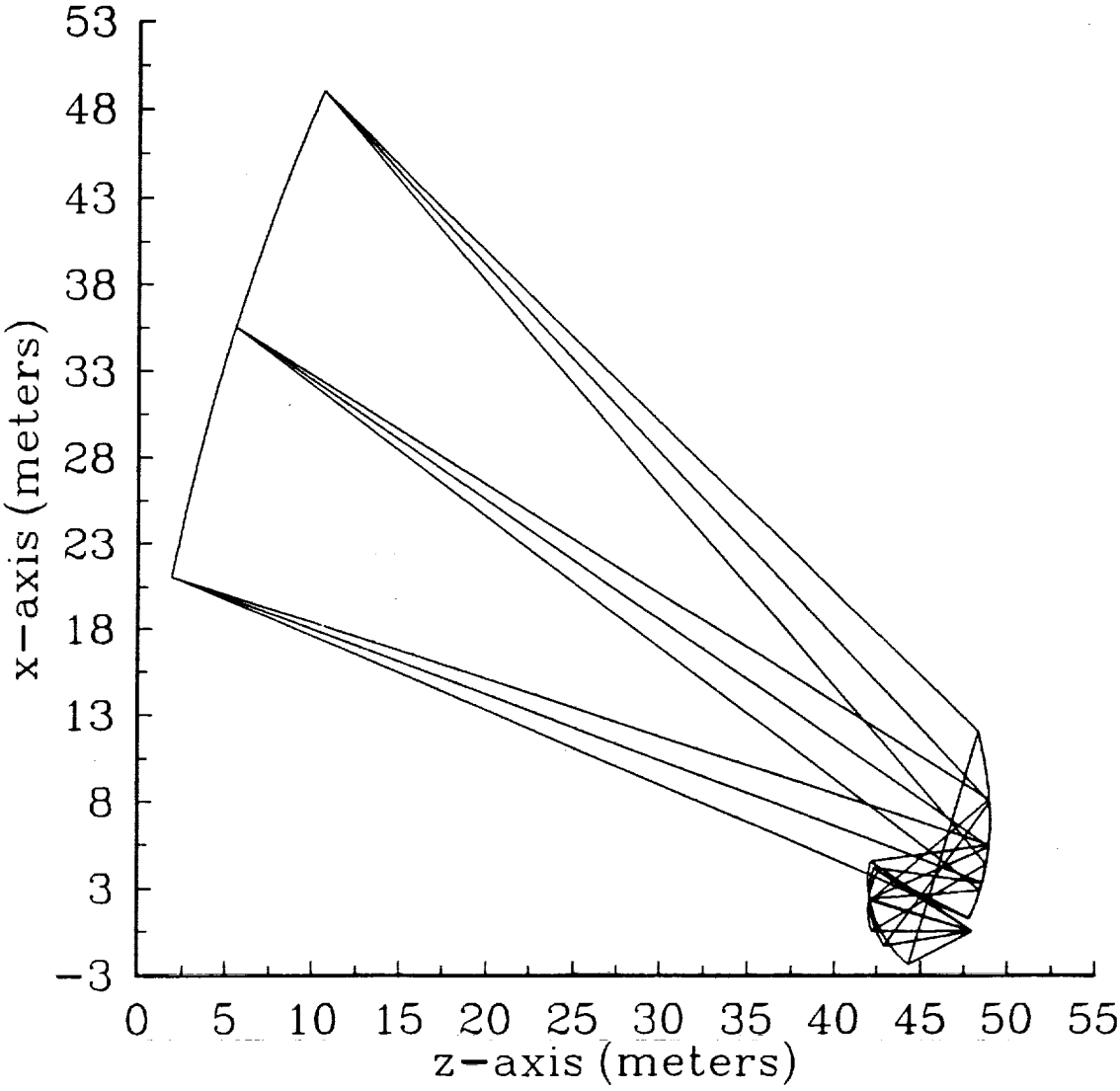

Figure 3.2-1. Foldes Type 2 (Cassegrain) reflector antenna configuration designed to scan ± 2.5°. Main reflector diameter is 28 m, main reflector focal length is 56 m (F/D=2). Elliptic subreflector diameter is 10.5 m. Shaped tertiary reflector diameter varies from 3.5 m to 6.7 m.

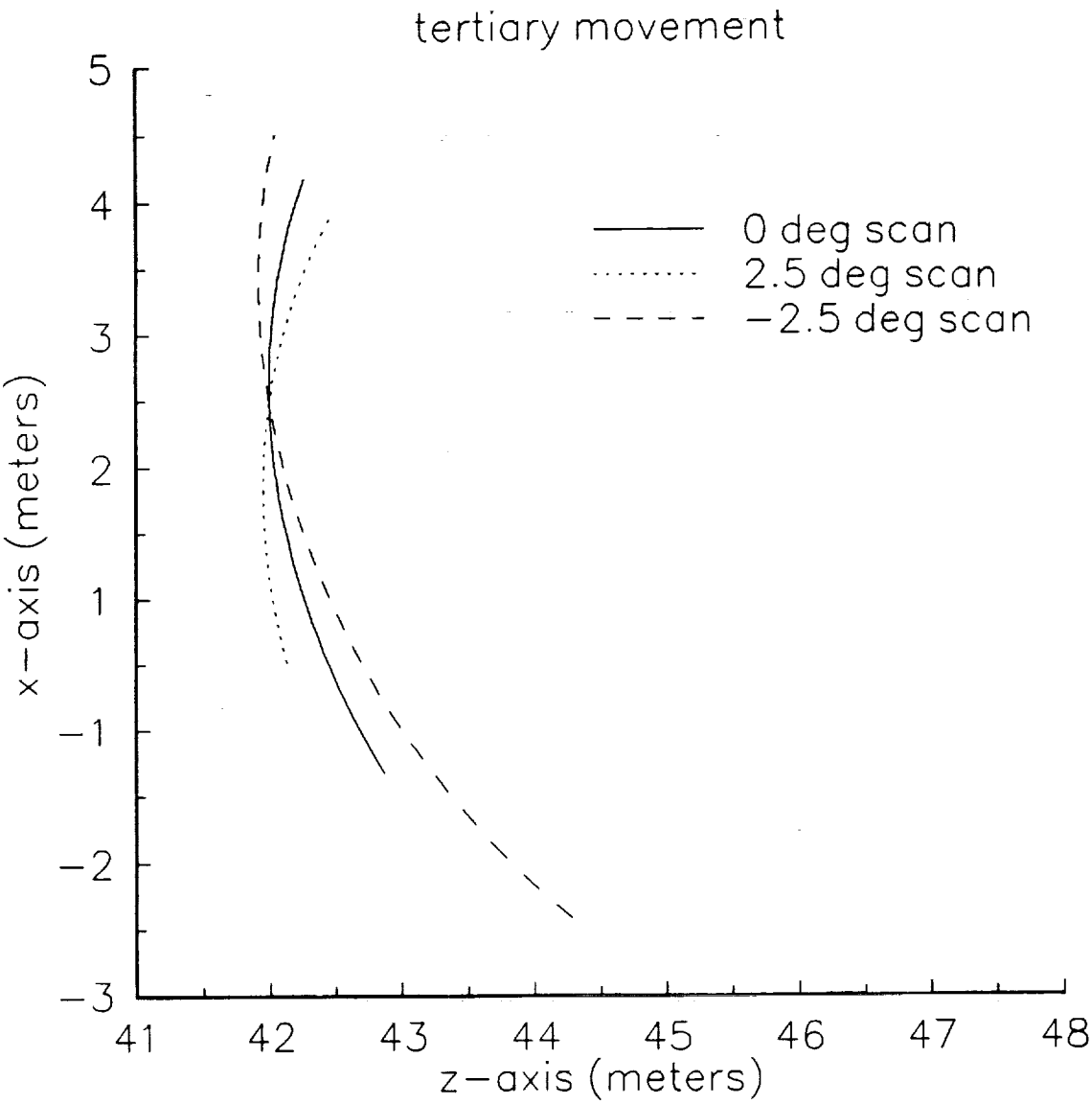

Figure 3.2-2. Tertiary reflector positions, sizes, and shapes for the Foldes Type 2 reflector (see Fig. 3.2-1) for the scan angles of +2.5°, 0°, and -2.5°.

directions are shown in Figs. 3.2-3 through 3.2-5. The patterns are poor with high sidelobes blended into the main beam and very shallow nulls between sidelobes. The probable cause for the poor patterns is an uneven amplitude distribution across the aperture of the main reflector. This problem is observed from Fig. 3.2-1 where ray paths for the +2.5°, 0° and -2.5° scan directions are drawn for rays striking the top, center and bottom of the main reflector. Corresponding to each these are three reflected rays: the top ray corresponding to the -2.5° scan direction, the middle ray corresponding to the 0° scan direction and the bottom ray corresponding to the +2.5° scan direction. Following these rays through the reflecting system, it becomes apparent that for each scan direction, the rays striking the tertiary are unevenly spaced (i.e., an unsymmetric illumination of the tertiary results from a symmetric illumination of the main reflector). That is, the points where the center ray and top ray intersect the tertiary are closer together than the points where the center ray and bottom ray intersect the tertiary (for each scan angle). Therefore, if one views the reflector configuration in a transmission mode, one would expect that if the tertiary were illuminated with a symmetric illumination the resulting main reflector illumination would be unsymmetric. This theory will hopefully be confirmed soon with the inclusion of an aperture field routine in MRAPCA.

A separate problem with the Foldes Type 2 Cassegrain configuration is with the angle that the subreflector intersects the received ray bundle. Because the subreflector is tilted with respect to the path swept out by the focal point as the reflector is made to scan, it cannot be made to be as small as would be possible if the subreflector were parallel to the path swept out by the focal point.

A configuration which attempts to solve both the problems of uneven aperture distribution and increased subreflector size is the Gregorian Type 2A reflector configuration. This is shown in Fig. 3.2-6. Note that this configuration allows the subreflector to run parallel to the path swept out by the focal point during scan and also results in a more symmetric illumination of the tertiary for a given symmetric main reflector illumination. In Fig. 3.2-6, the main reflector diameter is 30 m with a focal length of 56 m (F/D = 1.9). The system, designed to scan ±2.5 degrees, has a subreflector diameter of 9.46 m. The minimum tertiary diameter, corresponding to the +2.5° scan direction, is 5.09 m. The maximum tertiary diameter, corresponding to the -2.5° scan direction is 6.56 m. The tertiary motions are shown in Fig. 3.2-7. Patterns were calculated at 10 GHz (corresponding to a main reflector diameter of 1000 λ) using MRAPCA. A $\cos^q(\theta)$ feed pattern was used with q being chosen to give a -10 dB tertiary edge illumination. A shaped tertiary was used to each scan angle. The patterns are shown in Figs. 3.2-8 through

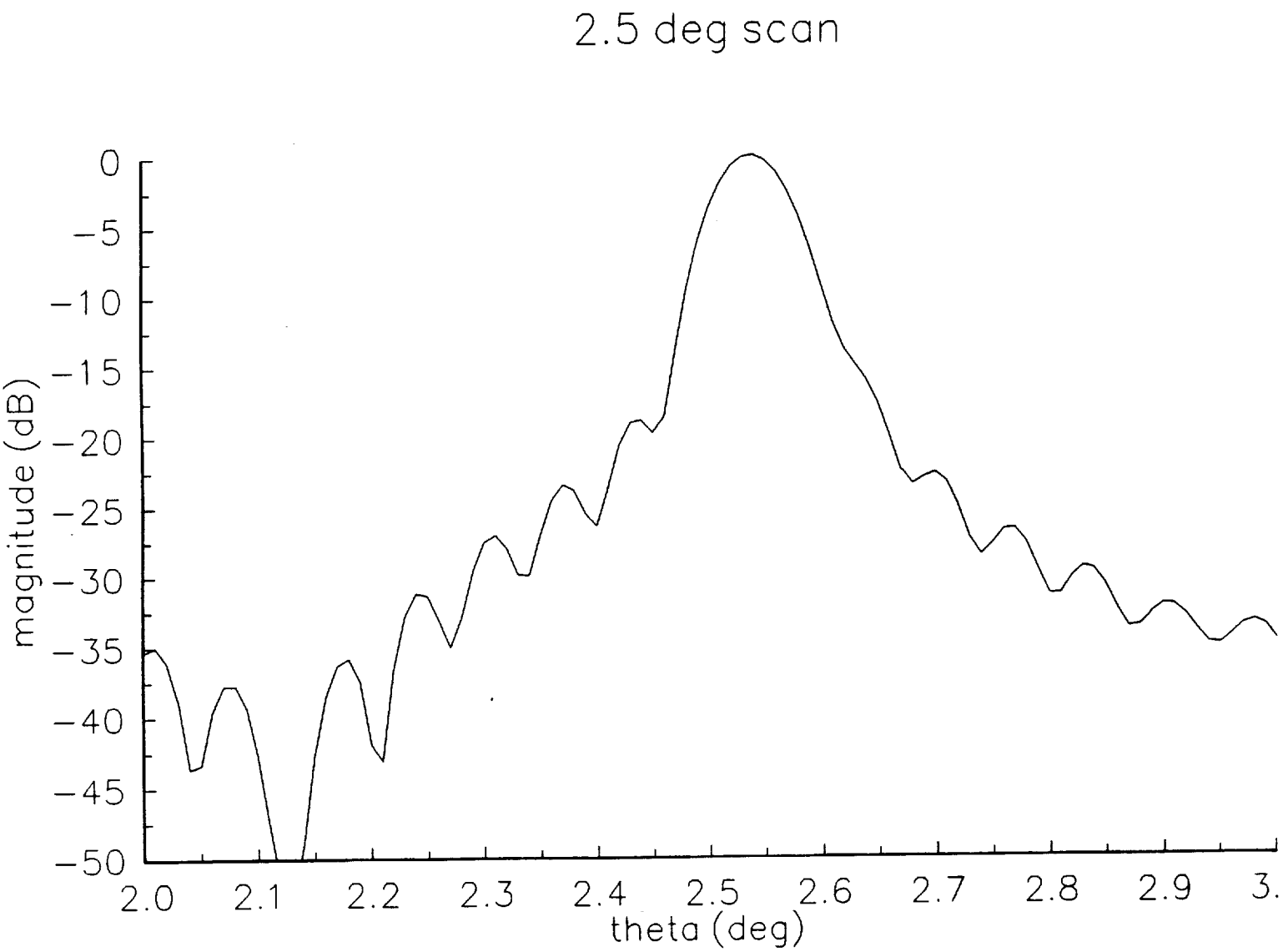

Figure 3.2-3. Radiation pattern of the Foldes Type 2 reflector antenna with correcting tertiary designed for the + 2.5° scan direction computed using MRAPCA. Feed pattern is $\cos^q(\theta)$ with q selected to give a -10 dB tertiary edge illumination. Main reflector diameter is 933 λ.

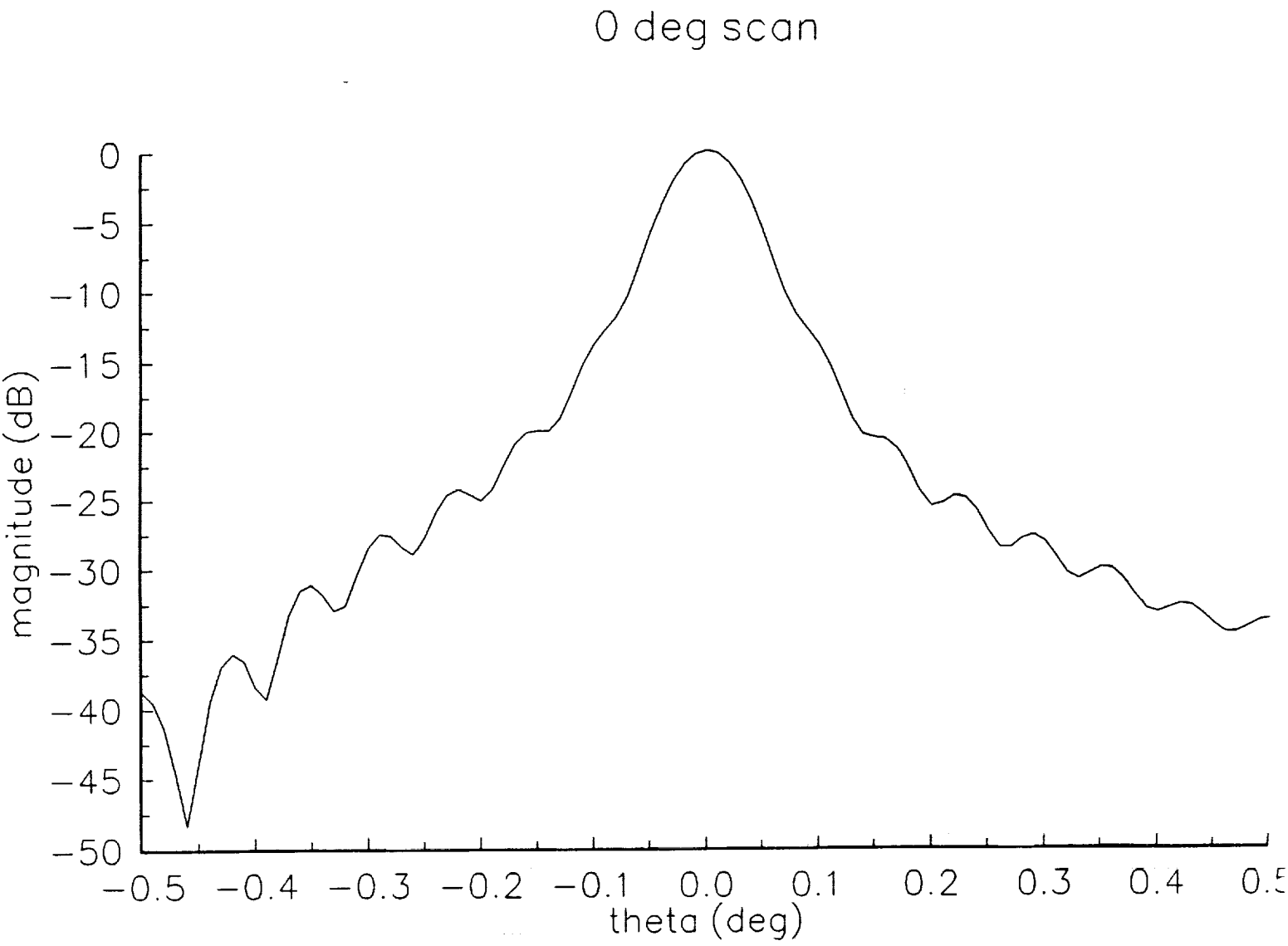

Figure 3.2-4. Radiation pattern of the Foldes Type 2 reflector antenna with correcting tertiary designed for the 0° scan direction computed using MRAPCA. Feed pattern is $\cos^q(\theta)$ with q selected to give a -10 dB tertiary edge illumination. Main reflector diameter is 933 λ

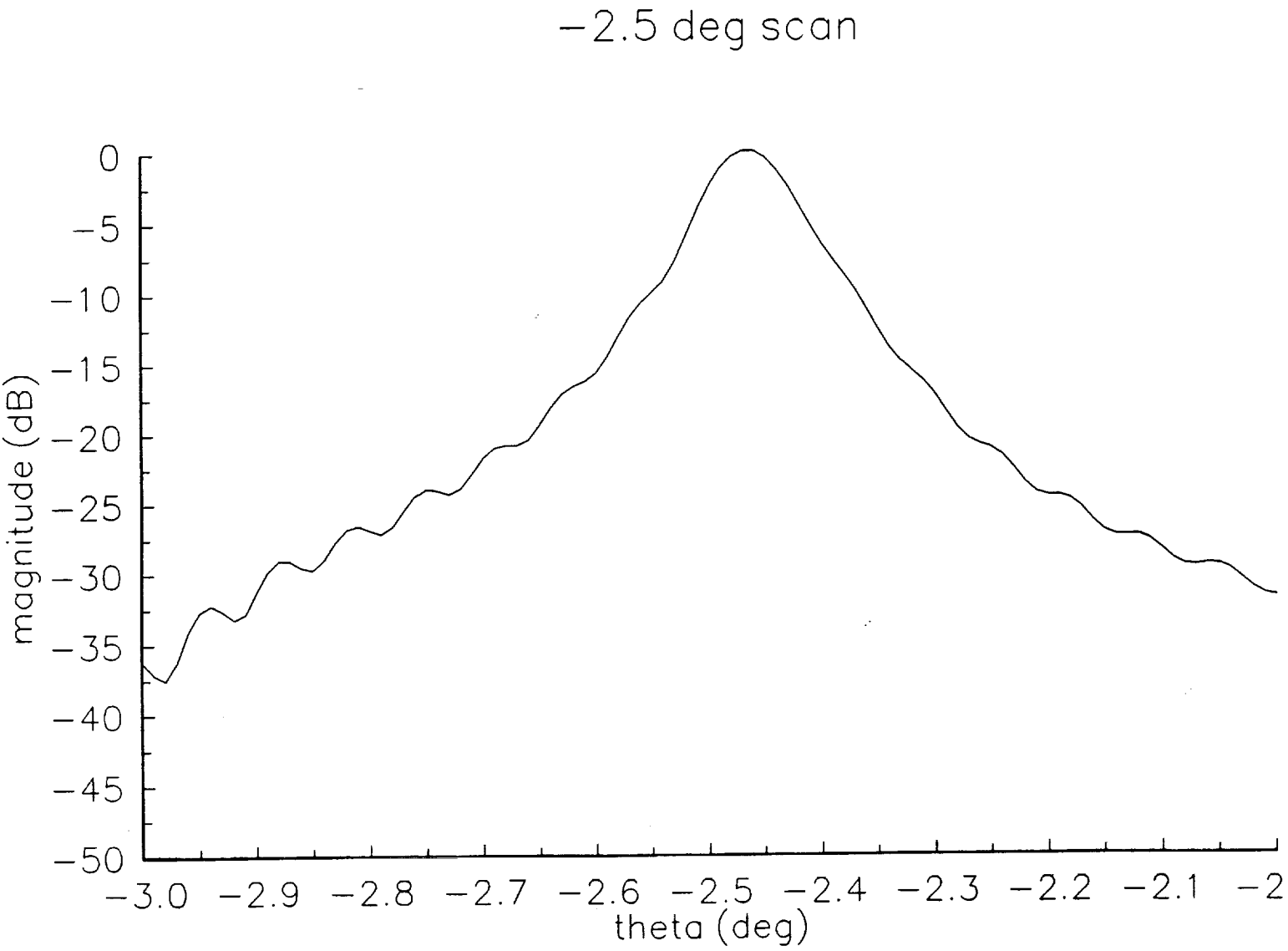

Figure 3.2-5. Radiation pattern of the Foldes Type 2 reflector antenna with correcting tertiary designed for the -2.5° scan direction computed using MRAPCA. Feed pattern is $\cos^q(\theta)$ with q selected to give a -10 dB tertiary edge illumination. Main reflector diameter is 933 λ

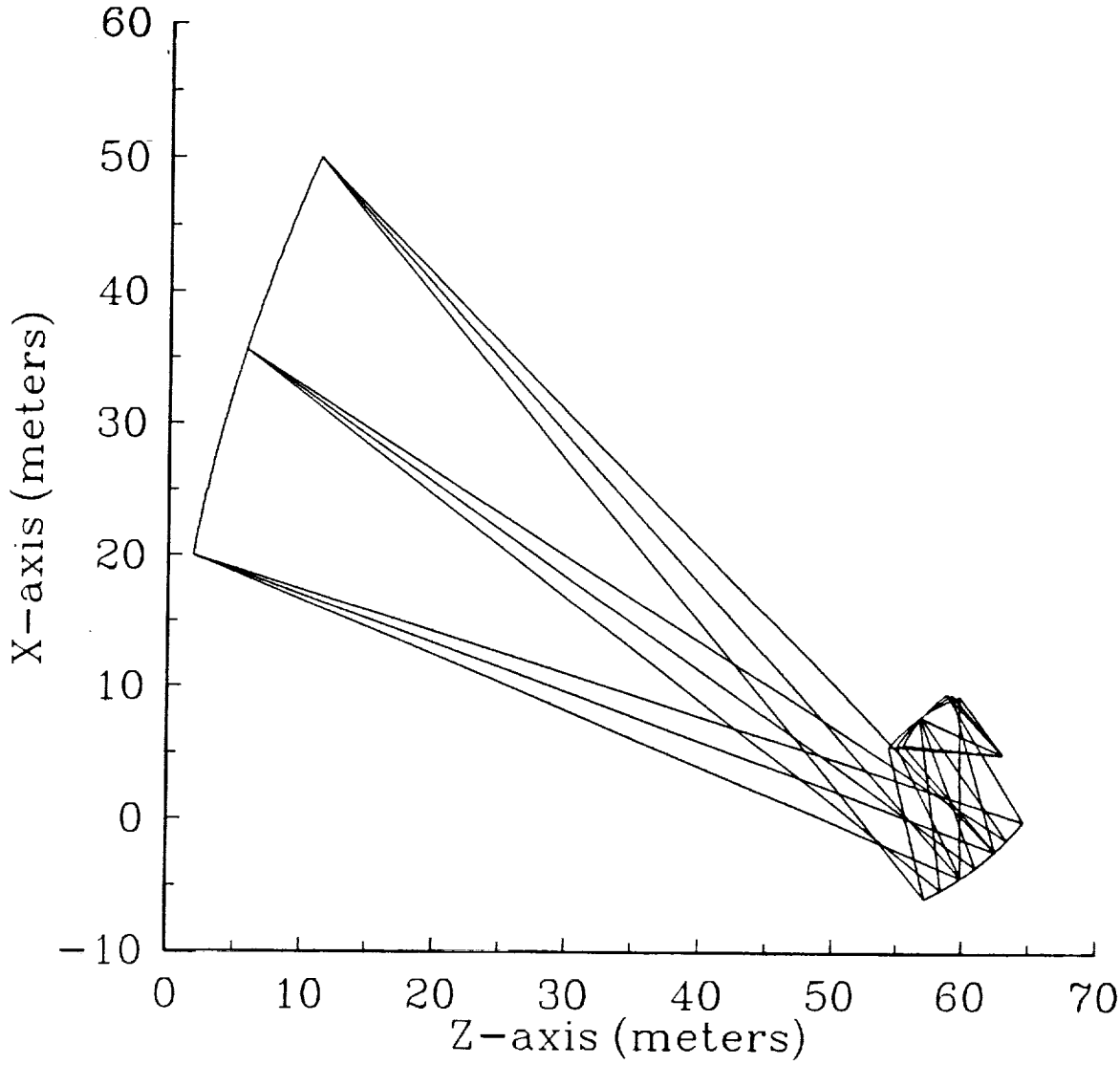

Figure 3.2-6. Gregorian Type 2A reflector antenna configuration designed to scan ± 2.5°. Main reflector diameter is 30 m, main reflector focal length is 56 m (F/D = 1.9). Elliptic subreflector diameter is 9.46 m. Shaped tertiary reflector diameter varies from 5.09 m to 6.56 m.

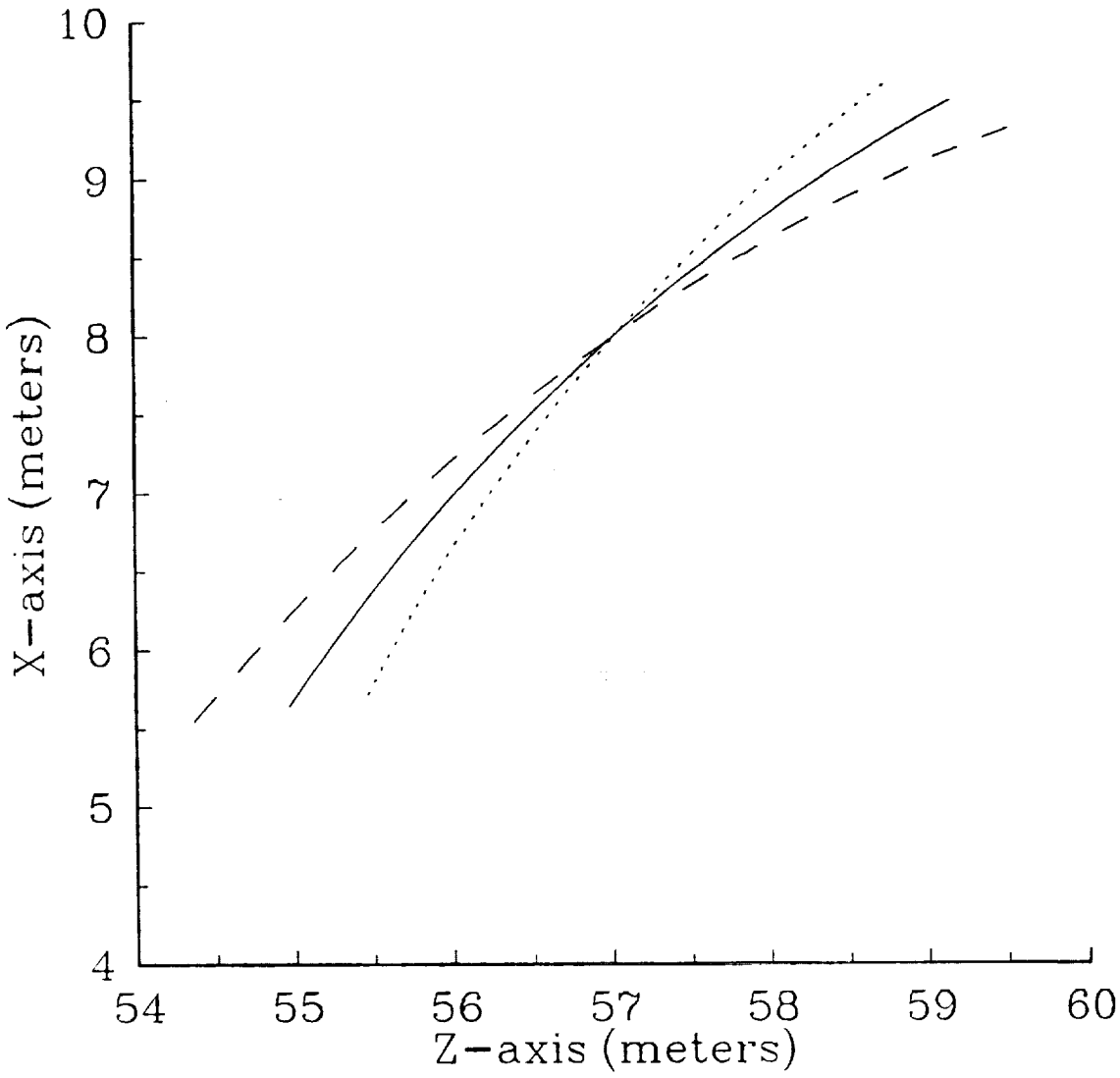

Figure 3.2-7. Tertiary reflector positions, sizes, and shapes for Gregorian Type 2A reflector system (see Fig. 3.2-6) for the scan angles of +2.5°, 0°, and -2.5°.

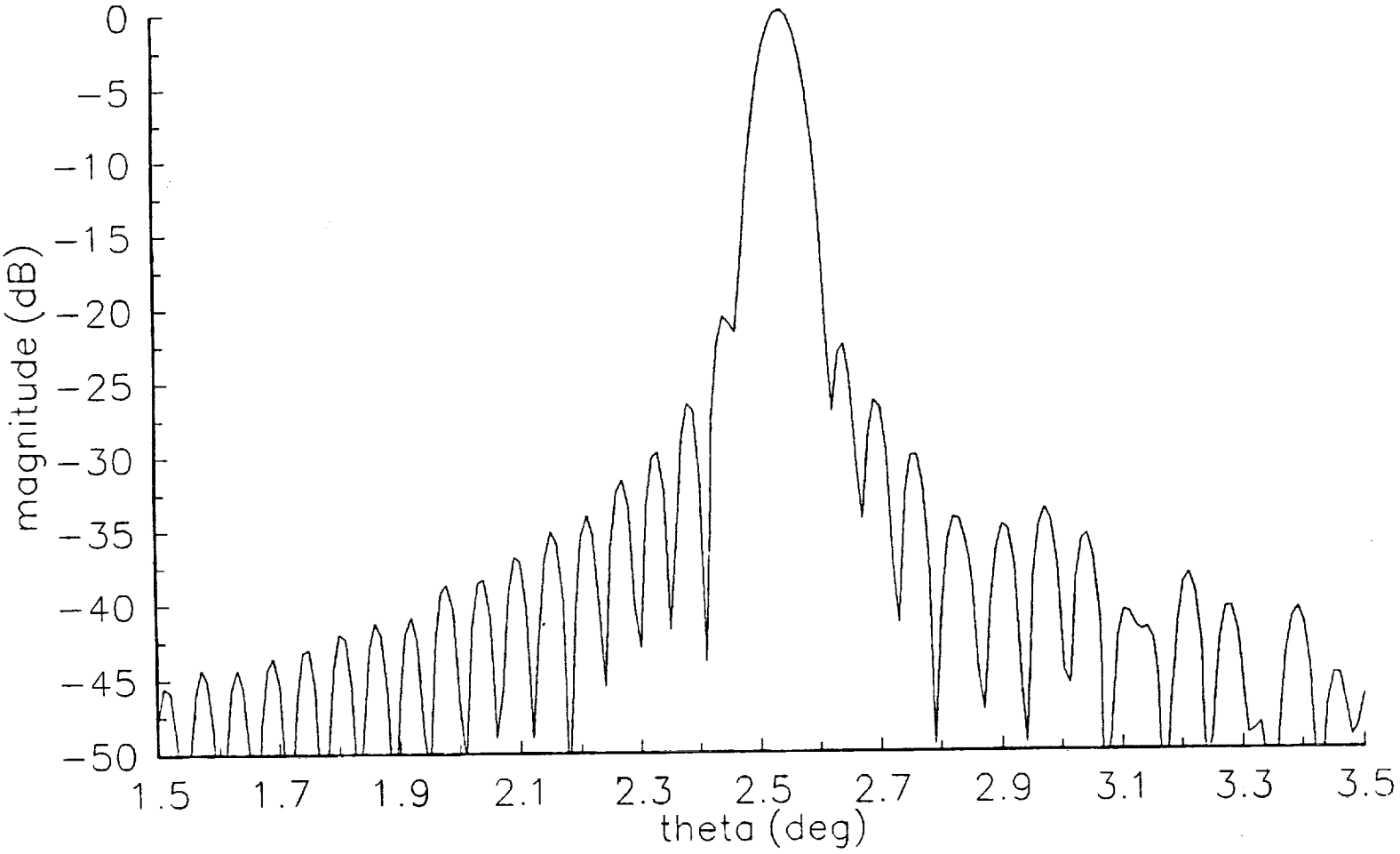

Figure 3.2-8 Radiation pattern of the Gregorian Type 2A reflector antenna with correcting tertiary designed for the + 2.5° scan direction computed using MRAPCA. Feed pattern is $\cos^q(\theta)$ with q selected to give a -10 dB tertiary edge illumination. Main reflector diameter is 1000 λ.

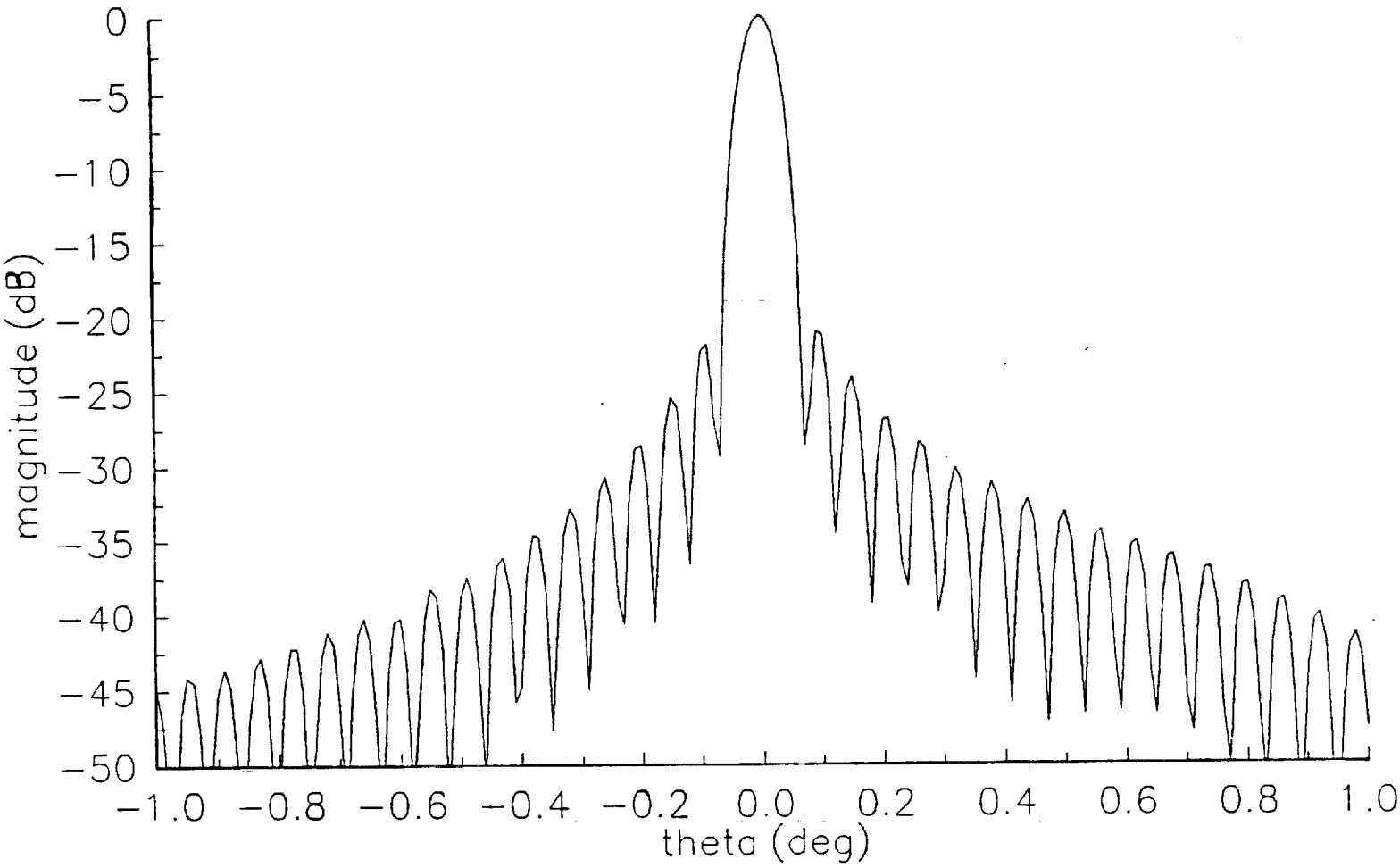

Figure 3.2-9 Radiation pattern os the Gregorian type 2(a) reflector antenna with correcting tertiary designed for the 0° scan direction computed using MRAPCA. Feed pattern is $\cos^q(\theta)$ with q selected to give a -10 dB tertiary edge illumination. Main reflector diameter is 1000 λ

3.2-10. These patterns show considerable improvement over those calculated for the Cassegrain configuration of Fig. 3.2-1.

One problem with the antenna configuration shown in Fig. 3.2-6 is that it is much longer than the configuration shown in Fig. 3.2-1. To shorten the system to approximately the same length as the Cassegrain configuration, the main reflector focal length was reduced to 40 m (F/D = 1.33). The resulting antenna configuration, designed to scan ±5°, is shown in Fig. 3.2-11. This is referred to as the Gregorian Type 2B reflector antenna. The subreflector diameter is 14.62 m and the tertiary diameter varies from 6.13 m to 10.11 m with the larger tertiary diameter corresponding to the +5° direction of scan. Patterns were calculated at 10 GHz (corresponding to a main reflector diameter of 1000 λ) using MRAPCA. In this case the tertiary diameter was reduced to 6 m for all directions of scan and the $\cos^q(\theta)$ feed pattern was chosen to give a tertiary edge illumination of -15 dB. The tertiary motions are shown in Fig. 3.2-12. The radiation patterns, resulting from using a correcting 6 m tertiary for each scan direction, are shown in Figs. 3.2-13 to 3.2-17. The lower sidelobes and broader main beam, compared to Figs. 3.2-3 through 3.2-5, are partially due to the higher edge taper and partially due to the fact that the main reflector is somewhat under illuminated for the positive directions of scan due to the 6 m limit on the tertiary diameter.

Finally, patterns were calculated for the Gregorian Type 2B antenna using a rotated (but not shaped) tertiary. The tertiary used was that calculated for the 0° scan direction and truncated to a diameter of 6 m. Patterns were calculated at 1 GHz, 2 GHz and 4 GHz (corresponding to a main reflector diameter of 100 λ, 200 λ and 400 λ) using MRAPCA for a $\cos^q(\theta)$ feed pattern selected to give a -15 dB tertiary edge illumination. These patterns are shown in Figs 3.2-18 through 3.2-20. At the higher frequencies the effects of a large amount of aperture phase error are clearly evident.

Future work includes the following:

1. Verifying the 2-D results for a full 3-D reflector system.

2. An investigation into the relationship between main reflector F/D ration, subreflector diameter and required tertiary shape correction for a given scan range (nominally ± 5°) for both the Cassegrain and Gregorian configurations.

3. An investigation into the possible array configurations for nonshape corrected tertiary reflectors.

4. An investigation into the feasibility of using a segmented dynamically shaped tertiary.

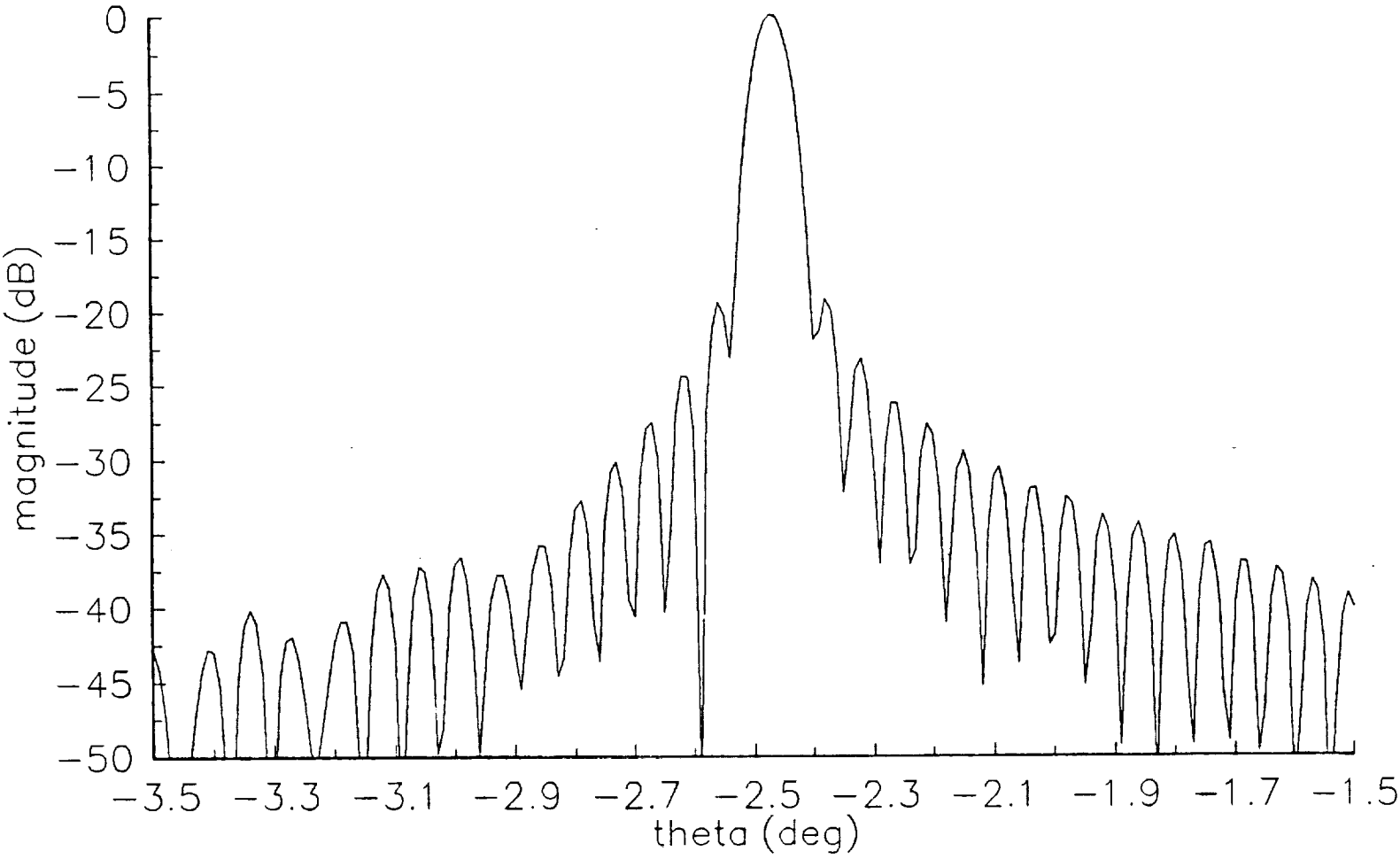

Figure 3.2-10. Radiation pattern of the Gregorian Type 2A reflector antenna with correcting tertiary designed for the -2.5° scan direction computed using MRAPCA. Feed pattern is $\cos^q(\theta)$ with q selected to give a -10 dB tertiary edge illumination. Main reflector diameter is 1000 λ.

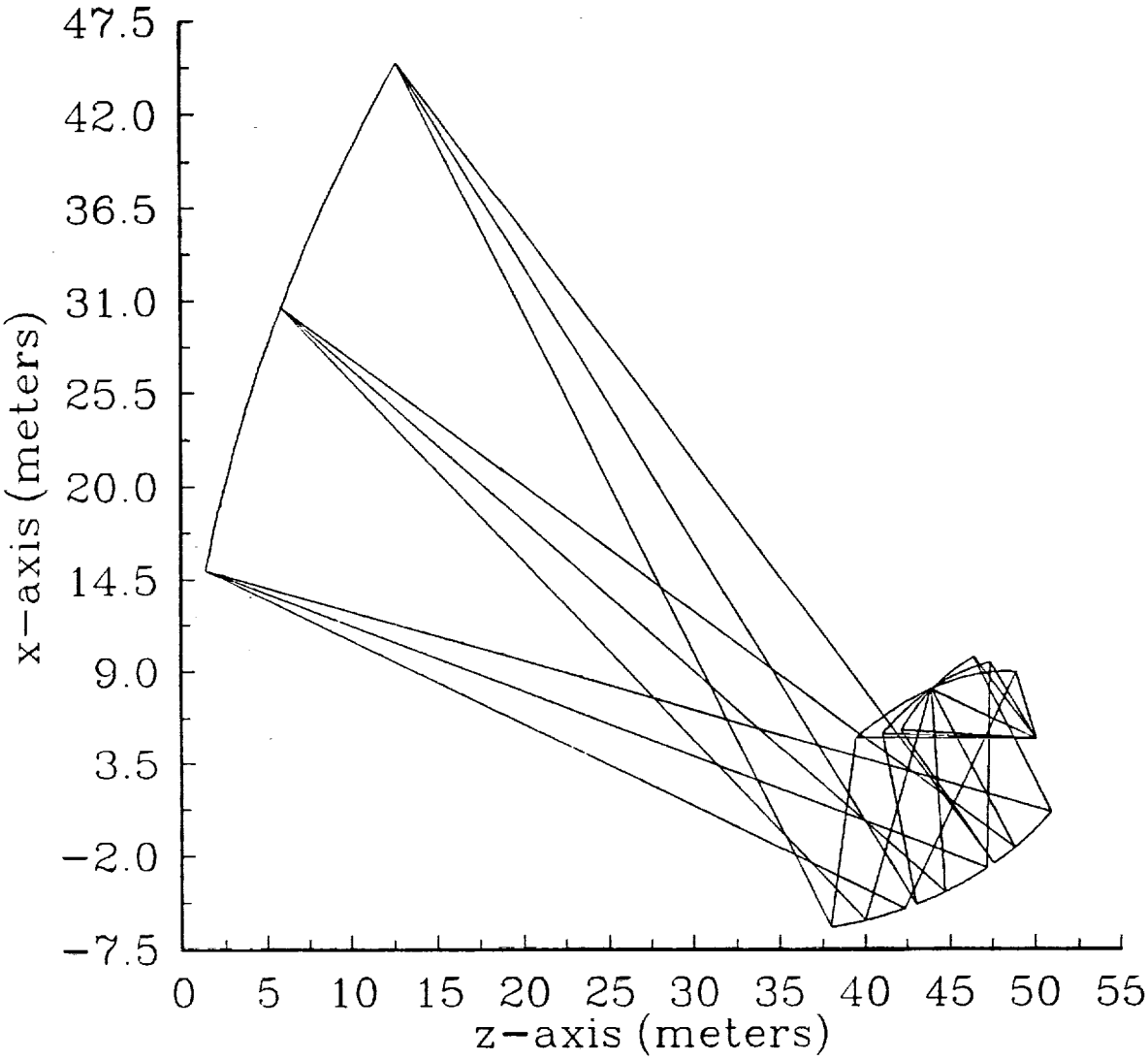

Figure 3.2-11. Gregorian Type 2B reflector antenna designed to scan ± 5°. Main reflector diameter is 30 m, main reflector focal length is 40 m (F/D = 1.333). elliptic subreflector diameter is 14.62 m. Shaped tertiary reflector diameter varies from 6.13 m to 10.11 m.

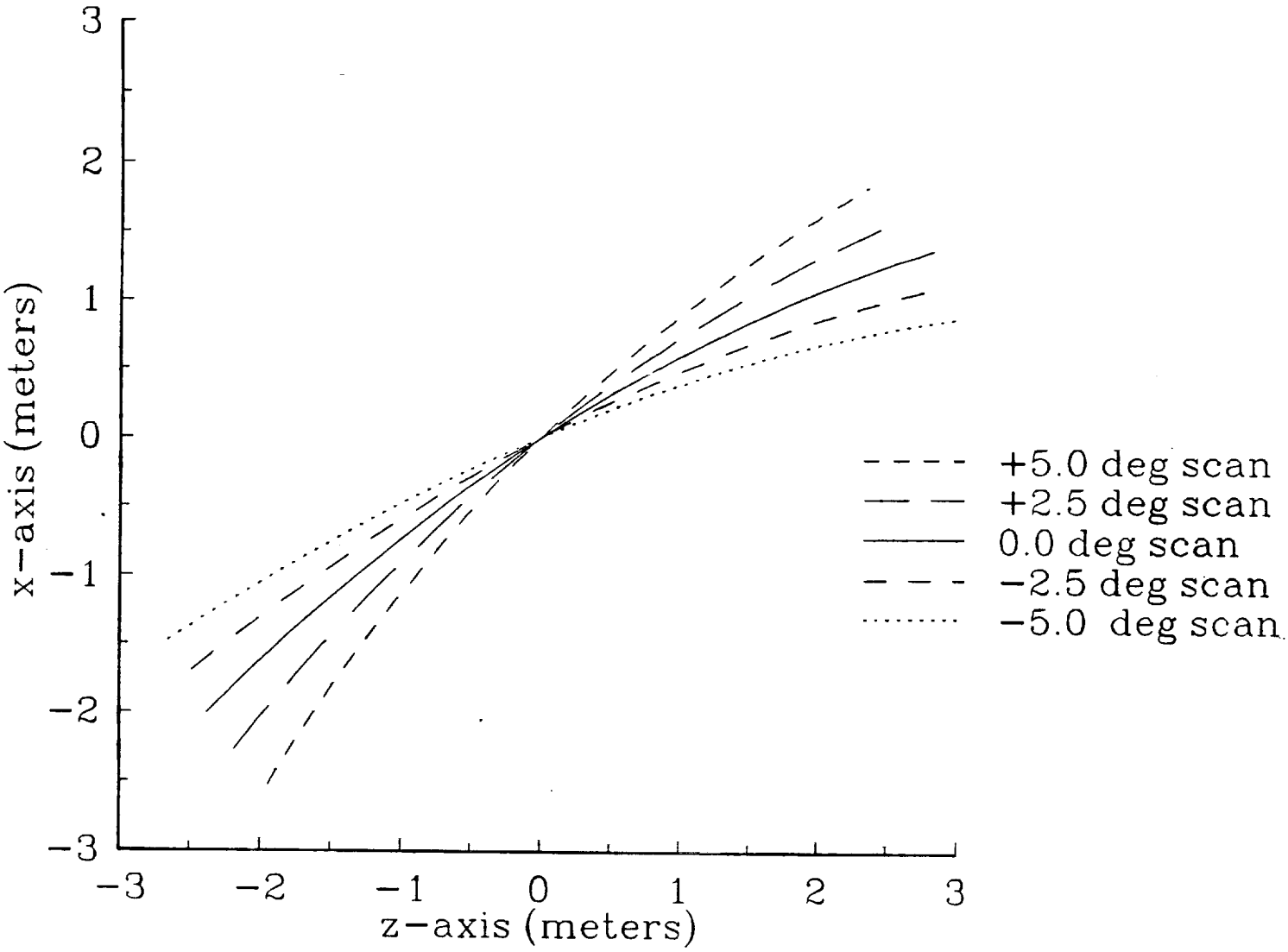

Figure 3.2-12. Tertiary reflector positions and shapes for the Gregorian Type 2B reflector system (see Fig. 3.2-11) for scan angles of +5°, +2.5°, 0°, -2.5°, and -5°. All tertiary diameters reduced to approximately 6 m.

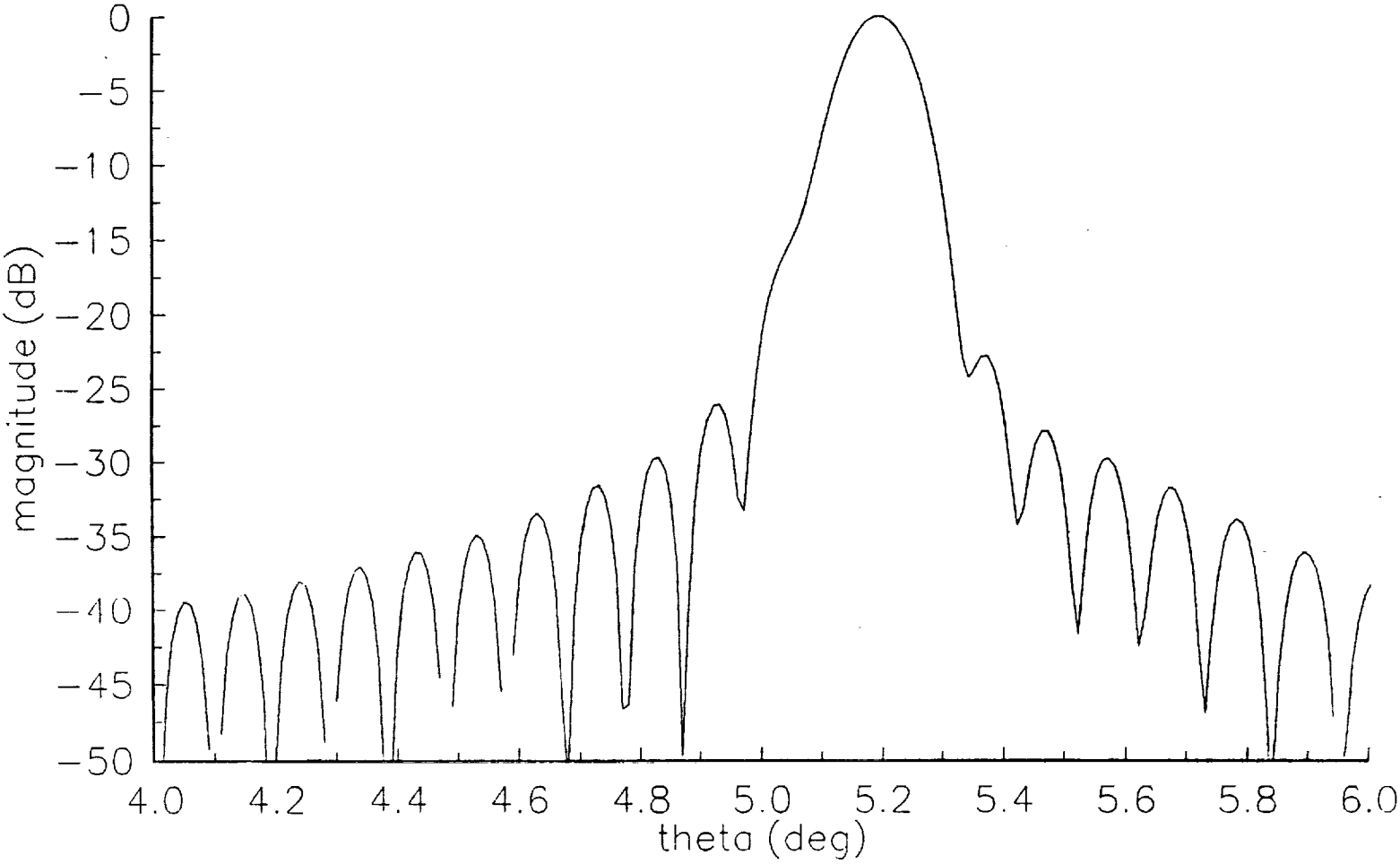

Figure 3.2-13. Radiation pattern of the Gregorian Type 2b reflector antenna with 5 m correcting tertiary designed for the +5 scan direction computed using MRAPCA. Feed pattern is $\cos^q(\theta)$ with q selected to give a -15 dB tertiary edge illumination. Main reflector diameter is 1000 λ.

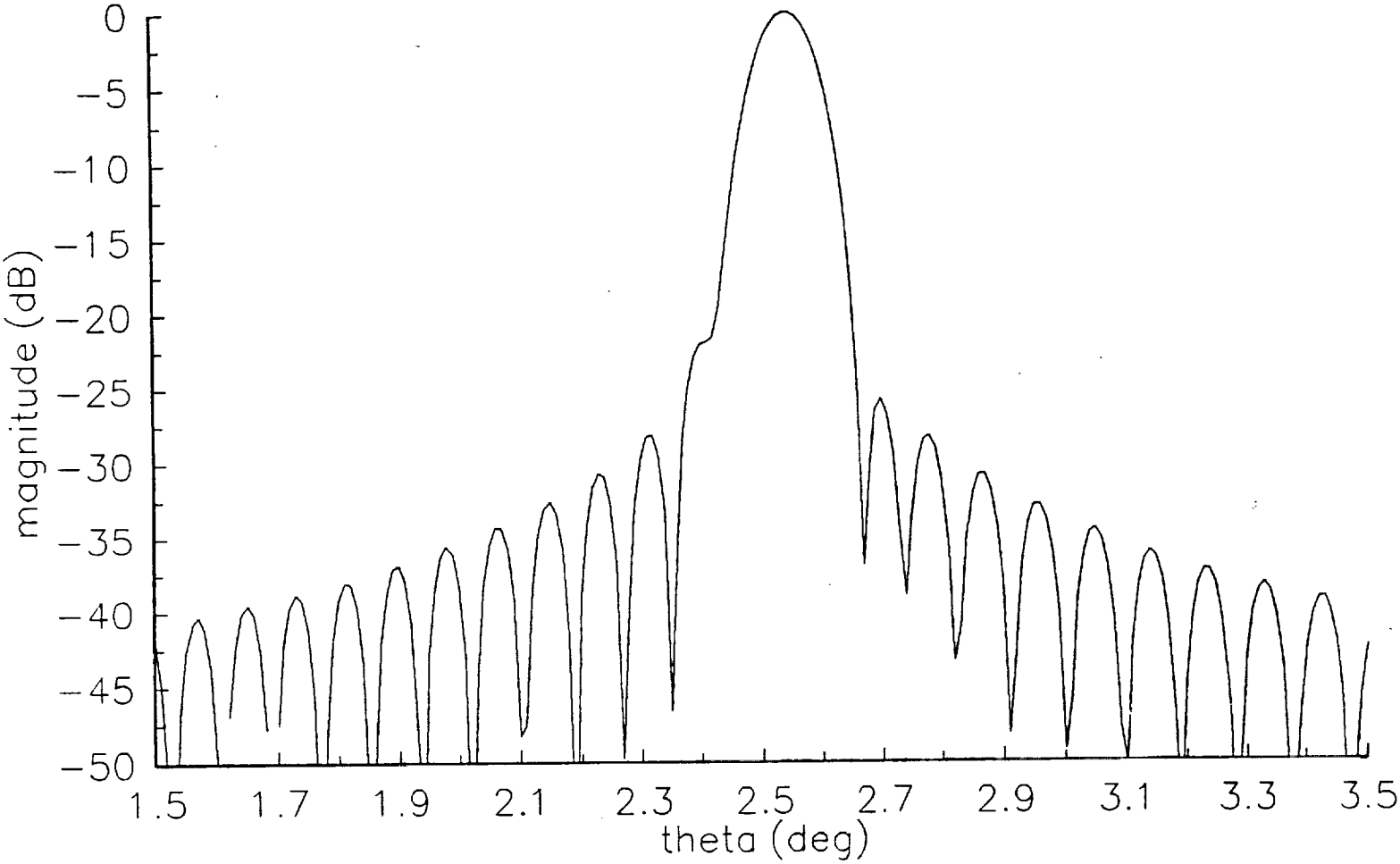

Figure 3.2-14. Radiation pattern of the Gregorian Type 2B reflector antenna with 6 m correcting tertiary designed for the +2.5° scan direction computed using MRAPCA. Feed pattern is $\cos^q(\theta)$ with q selected to give a -15 dB tertiary edge illumination. Main reflector diameter is 1000 λ.

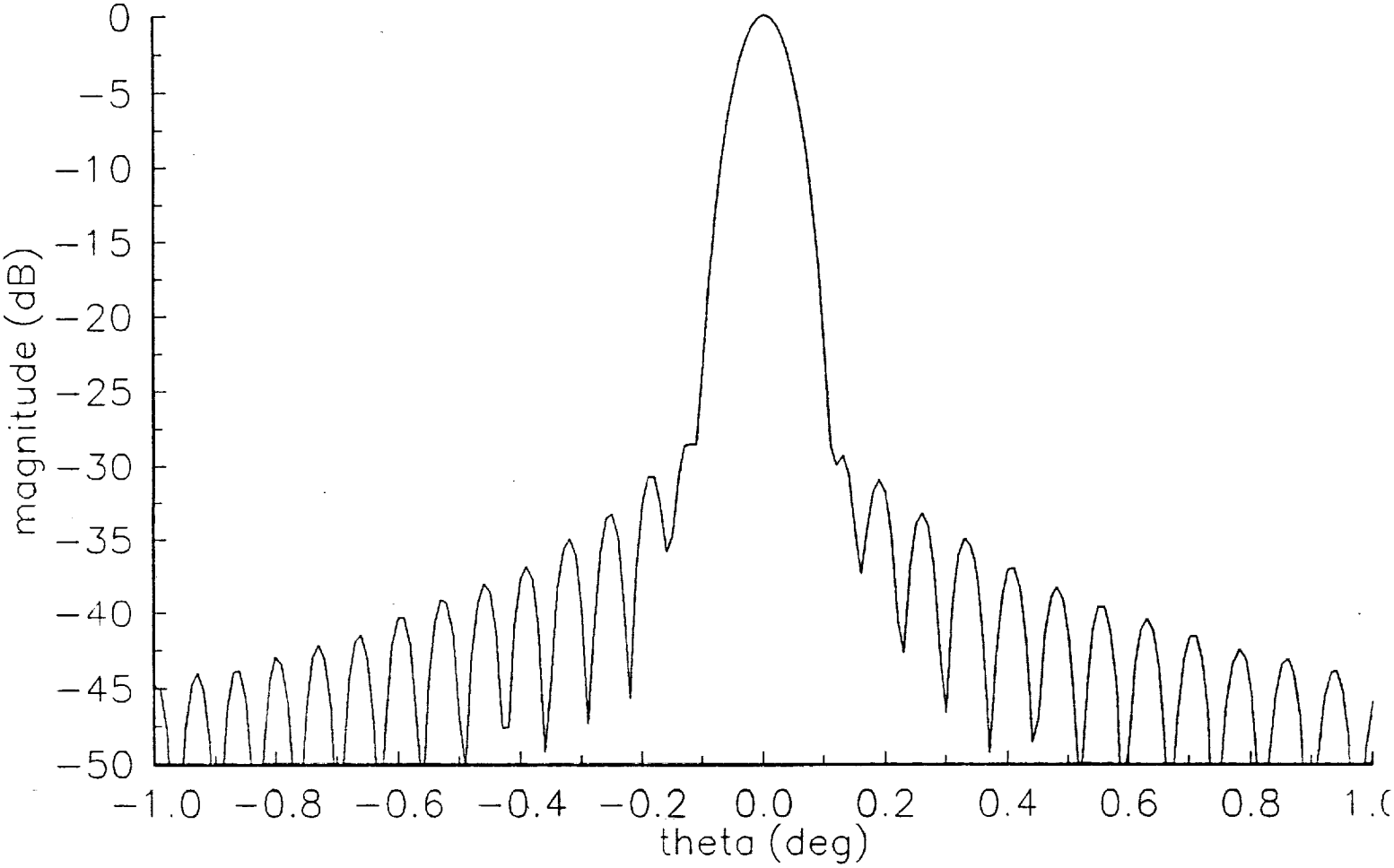

Figure 3.2-15. Radiation pattern of the Gregorian Type 2B reflector antenna with 6 m correcting tertiary designed for the +0° scan direction computed using MRAPCA. Feed pattern is $\cos^q(\theta)$ with q selected to give a -15 dB tertiary edge illumination. Main reflector diameter is 1000 λ.

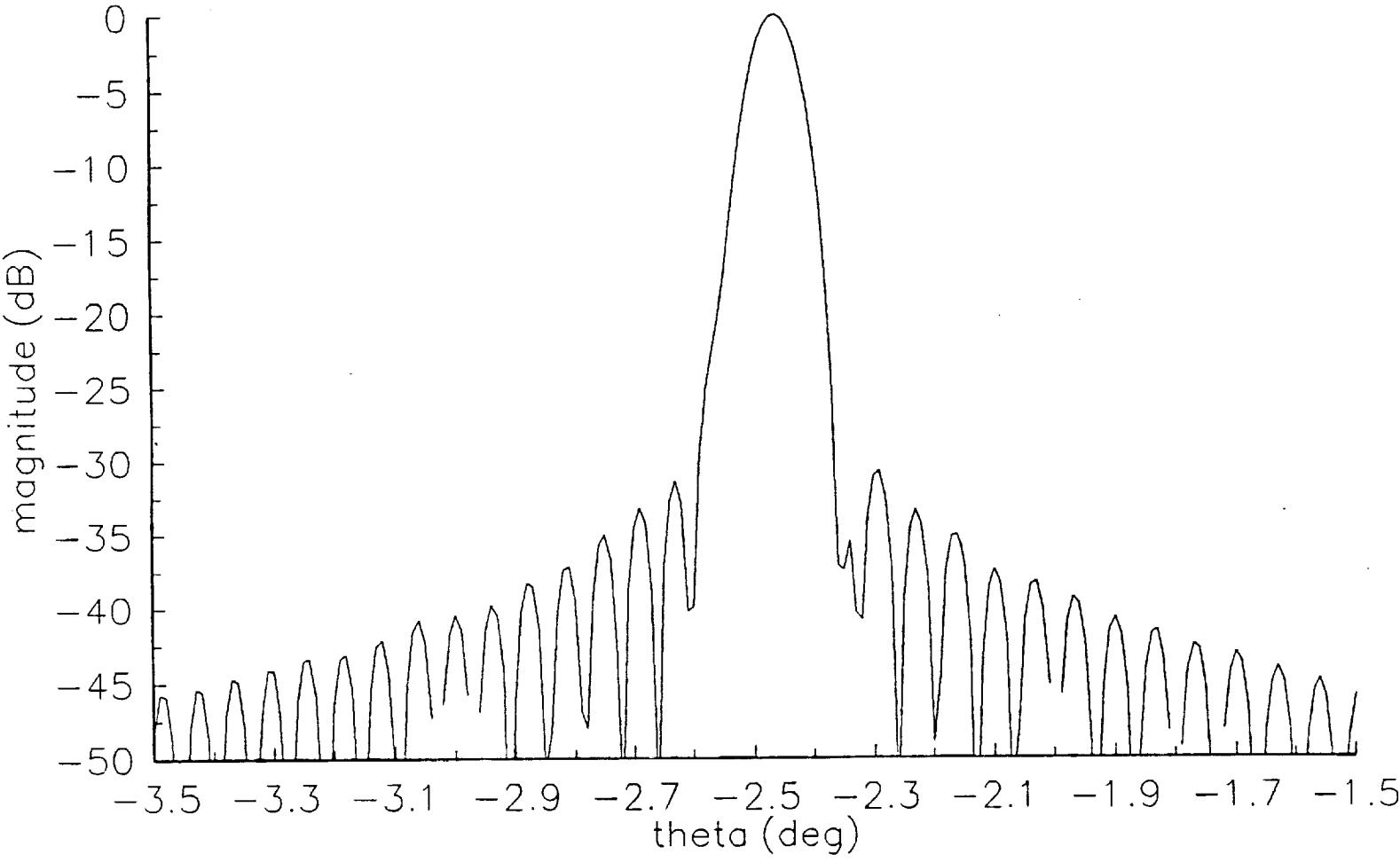

Figure 3.2-16. Radiation pattern of the Gregorian Type 2B reflector antenna with 6 m correcting tertiary designed for the -2.5° scan direction computed using MRAPCA. Feed pattern is $\cos^q(\theta)$ with q selected to give a -15 dB tertiary edge illumination. Main reflector diameter is 1000 λ.

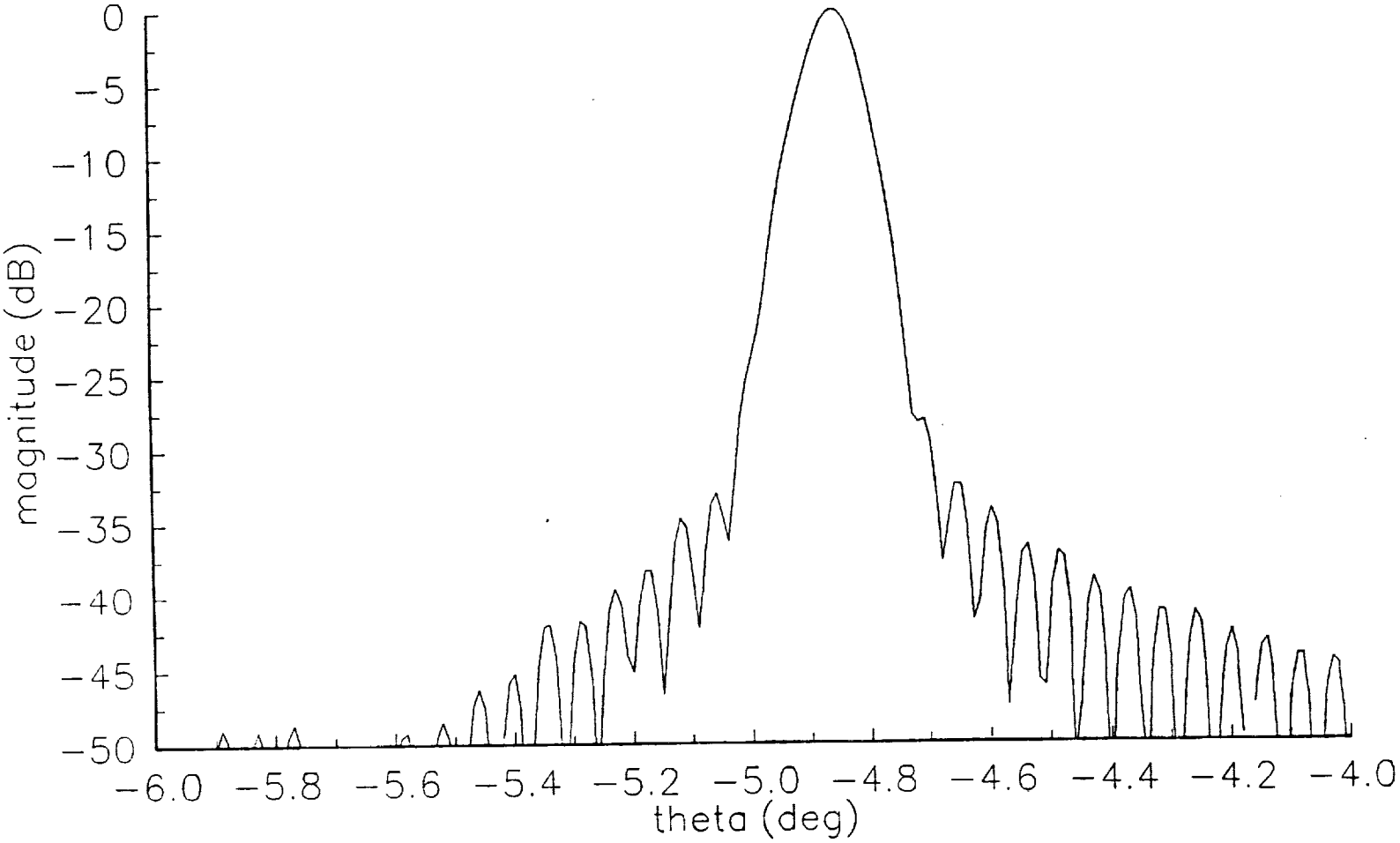

Figure 3.2-17. Radiation pattern of the Gregorian Type 2B reflector antenna with 6 m correcting tertiary designed for the -5° scan direction computed using MRAPCA. Feed pattern is $\cos^q(\theta)$ with q selected to give a -15 dB tertiary edge illumination. Main reflector diameter is 1000 λ.

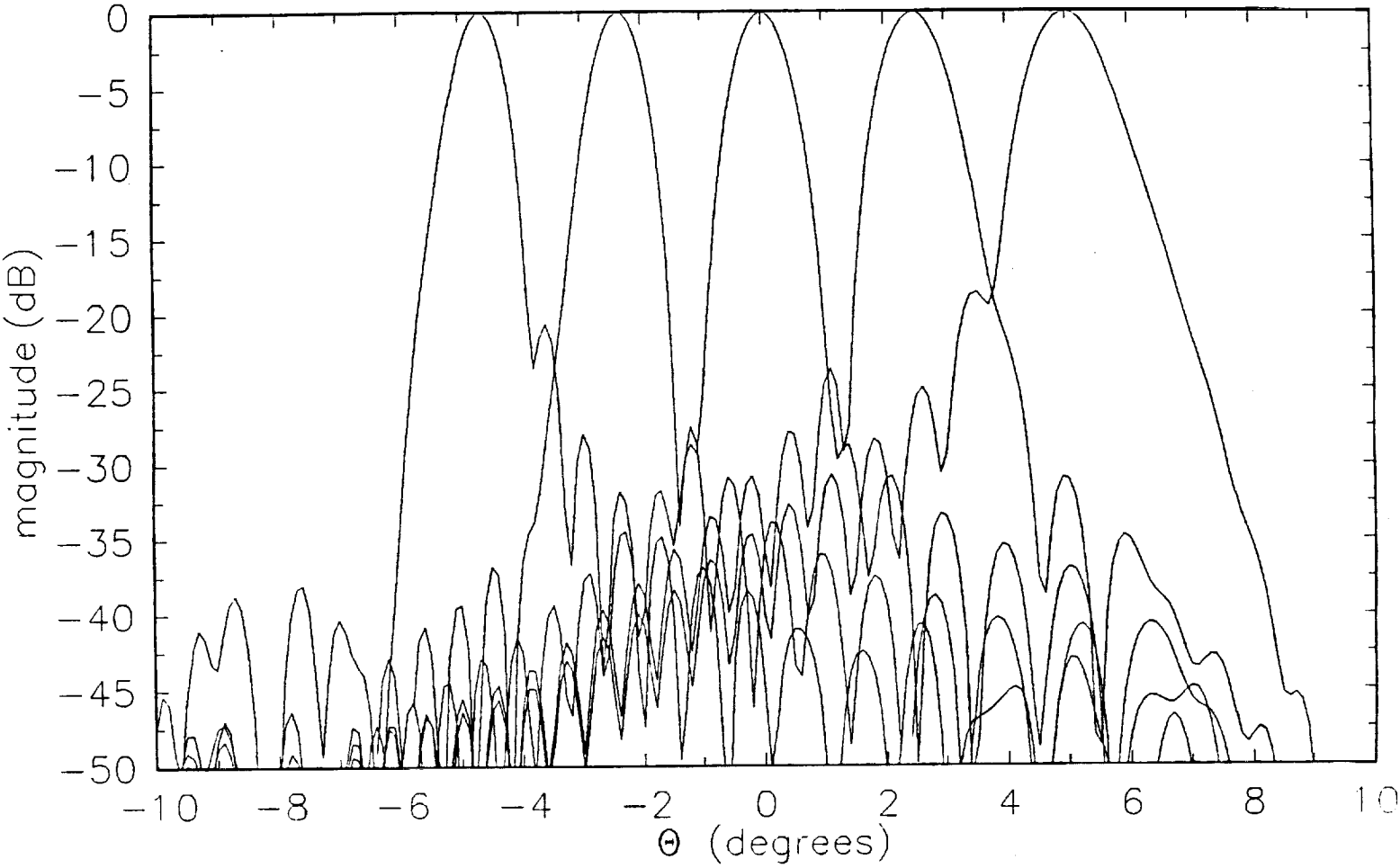

Figure 3.2-18. Radiation pattern of the Gregorian Type 2B reflector antenna with 6 m non-corrected tertiary designed for the 0° scan direction and rotated to obtain ± 5° scan computed using MRAPCA. Feed pattern is $\cos^q(\theta)$ with q selected to give a -15 dB tertiary edge illumination. Main reflector diameter is 100 λ.

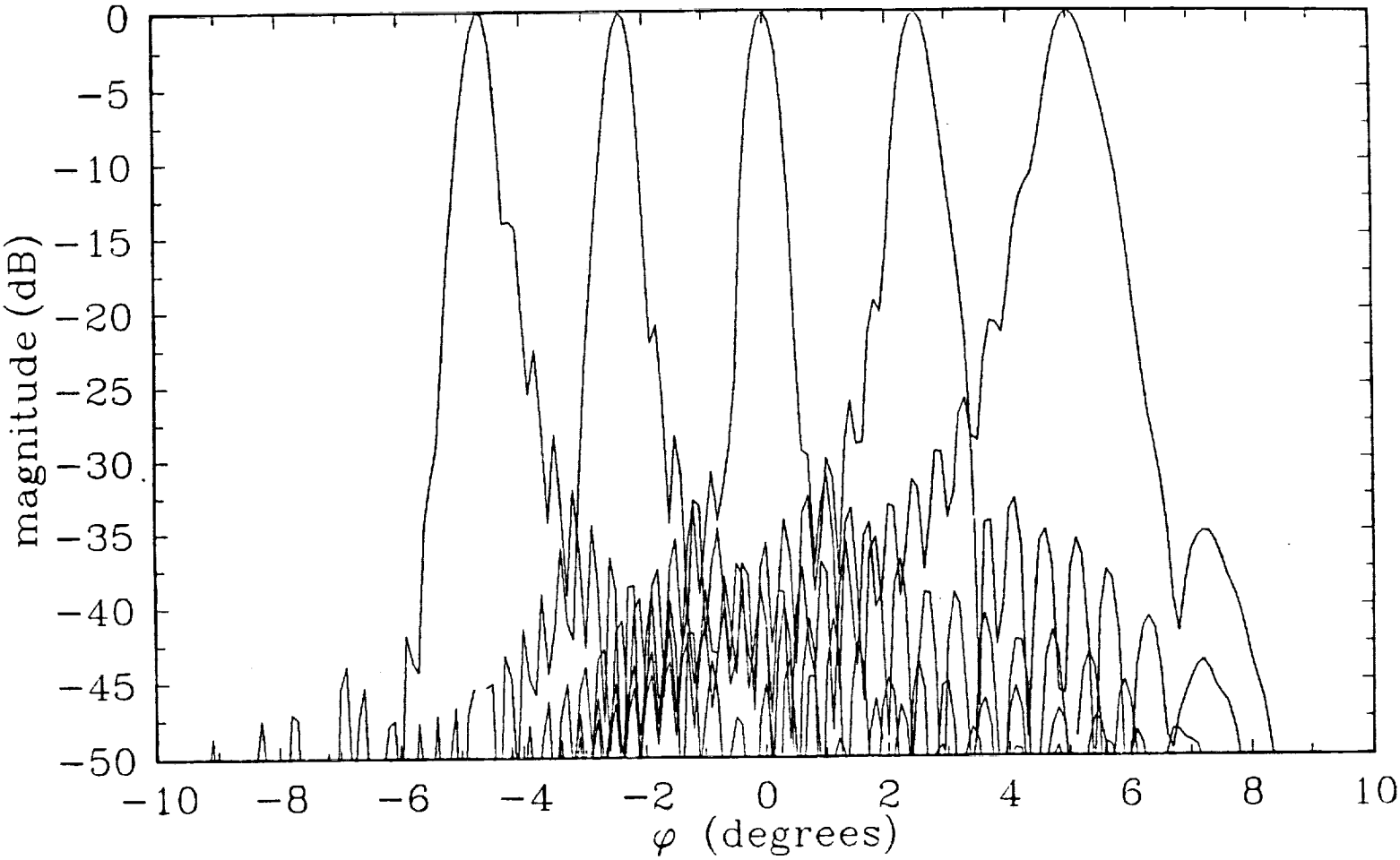

Figure 3.2-19. Radiation pattern of the Gregorian Type 2B reflector antenna with 6 m non-corrected tertiary designed for the 0° scan direction and rotated to obtain ± 5° scan computed using MRAPCA. Feed pattern is $\cos^q(\theta)$ with q selected to give a -15 dB tertiary edge illumination. Main reflector diameter is 200 λ.

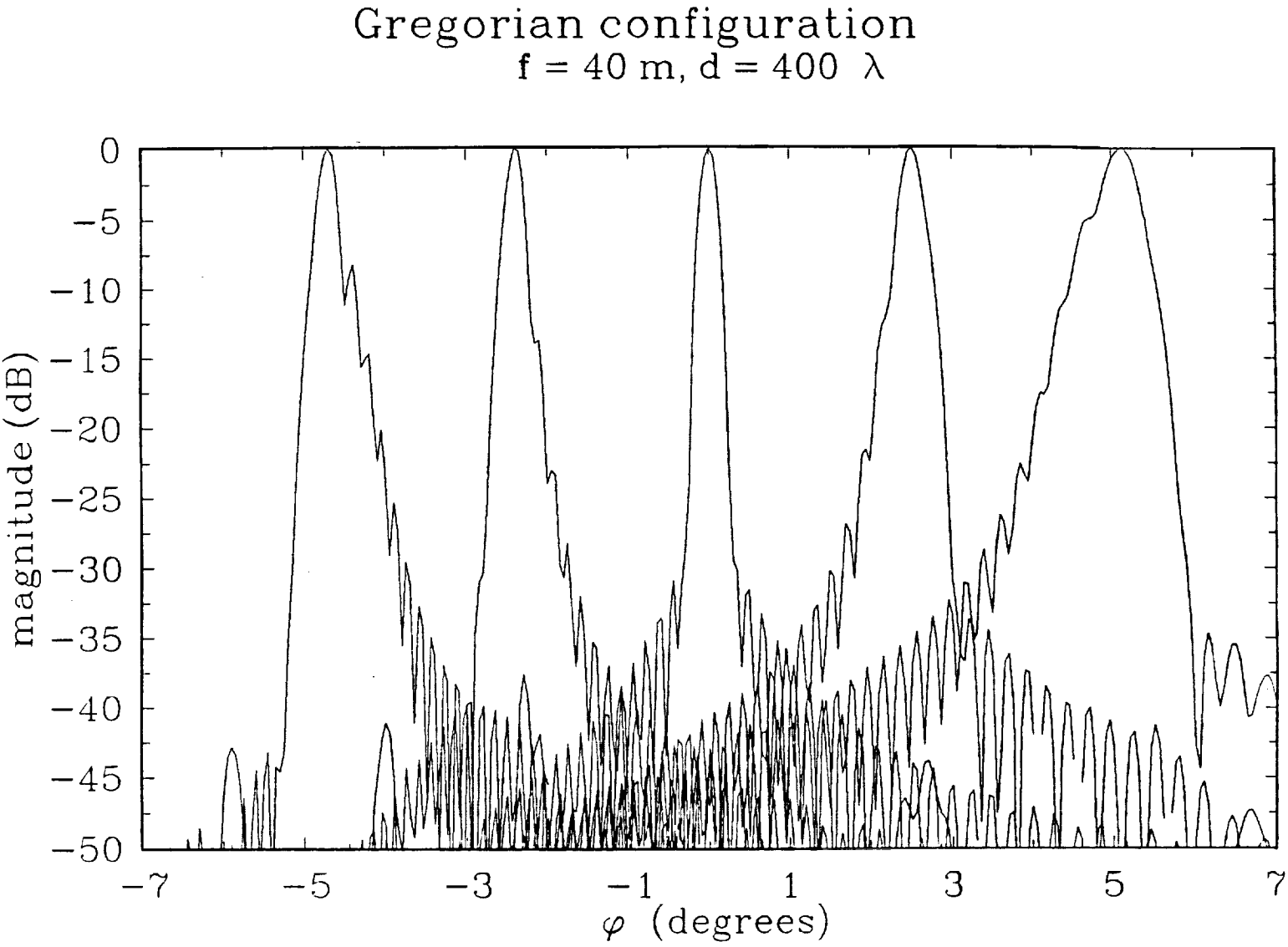

Figure 3.2-20. Radiation pattern of the Gregorian Type 2B reflector antenna with 6 m non-corrected tertiary designed for the 0° scan direction and rotated to obtain ± 5° scan computed using MRAPCA. Feed pattern is $\cos^q(\theta)$ with q selected to give a -15 dB tertiary edge illumination. Main reflector diameter is 400 λ.

5. An investigation into the possibility of using tertiary and feed translational movement to reduce the phase error of a fixed tertiary shape system.

3.3 Foldes Type 6 Reflector Systems

An in depth examination of the Foldes Type 6 reflector antenna configuration began in December 1990. Unlike previous investigations of the Type 6 configuration, this effort centers on determining the optimum scan path for a non-dynamically reshaping subreflector. Since this type of positioning results in the minimal subreflector surface error relative to a reshaping subreflector, the results of this study will also be useful in the design of reshaping systems because it will minimize the required active deformation. Currently, the two-dimensional case is under consideration and is being used to develop general algorithms.

The main difference between the previous dynamically reshaping subreflector analysis and the present effort is that the earlier work specified a total aperture-plane-to-feed path length and designed a subreflector to match. The current approach is to specify a subreflector and then find the optimum position for the given subreflector. Figures 3.3-1 to 3.3-3 show the algorithm components. An initial subreflector position is selected using geometric optics ray tracing to find the path length variance, and then moving the subreflector to a new position and recalculating the variance. This procedure is then repeated until the position with the minimum variance is found. Currently, the errors in the path length are unweighted but later calculations will include the effect of field taper over the antenna aperture. Preliminary results indicate subreflector motion is rotation of the subreflector about the feed location. Insights gained from this example will be used to guide selection of further investigations.

3.4 Spherical Reflector Systems

Spherical reflectors, when used in conjunction with one or more correcting subreflectors, offer the possibility of undistorted scanning without the need for a phased array feed. The penalty for being able to use a simple feed are: complicated motion of the feed and correcting reflector(s), and reduced main reflector aperture illumination efficiency. An example of the scanning scenario used for a spherical reflector fed by a movable feed and correcting reflector is shown in Fig. 3.4-1. The reflector is chosen to allow for ±5° of scan with no spillover. Rays are drawn representing the edge rays for which the spillover boundary is defined. The solid rays correspond to the 0° scan direction while the dashed rays correspond to the +5° scan direction. Notice, for this case there is no relative motion between the feed and correcting subreflector and the two move as

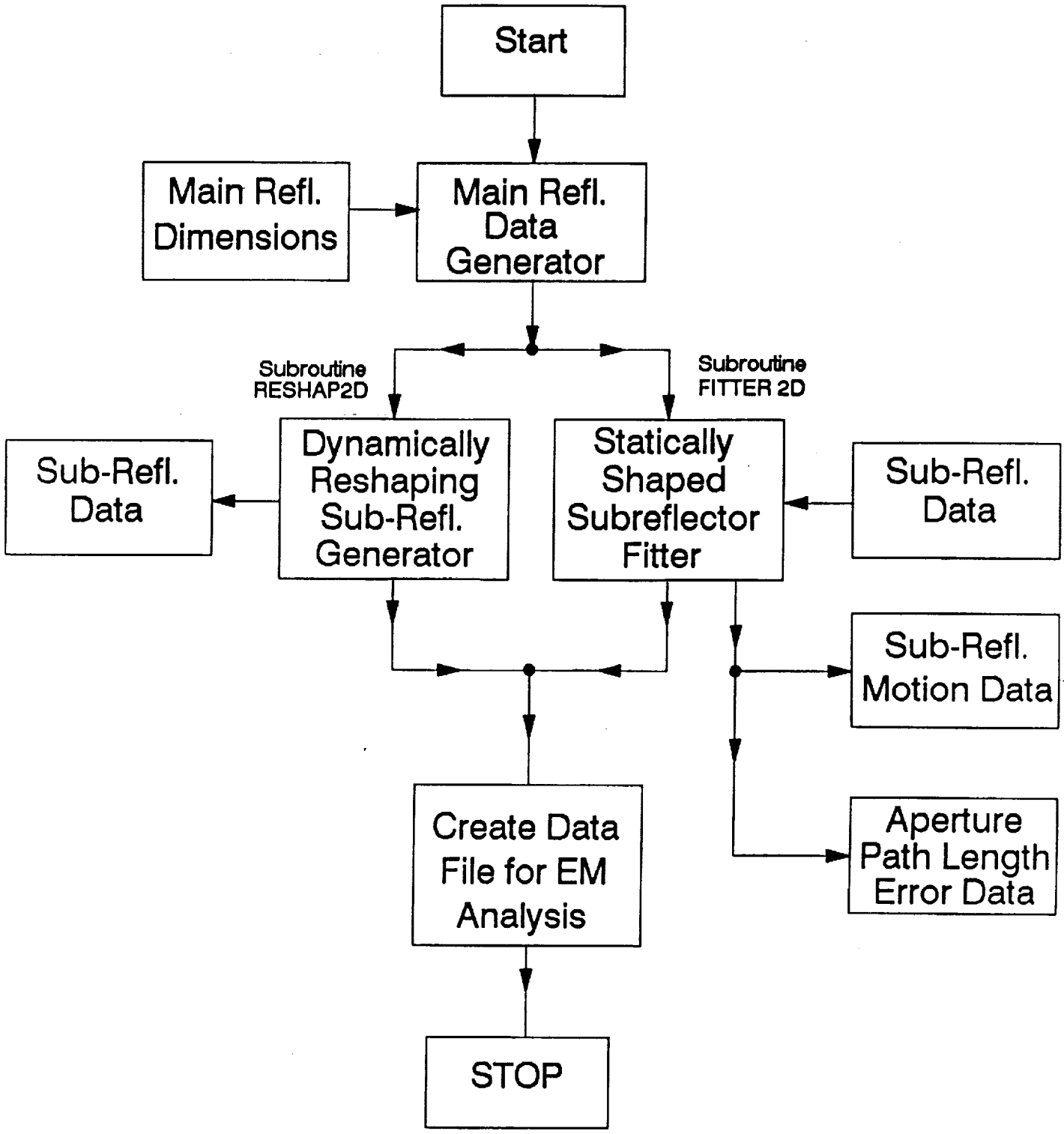

Figure 3.3-1 Subreflector Scan Movement Optimization Code - 2D (SSMOC) Data Flow Chart.

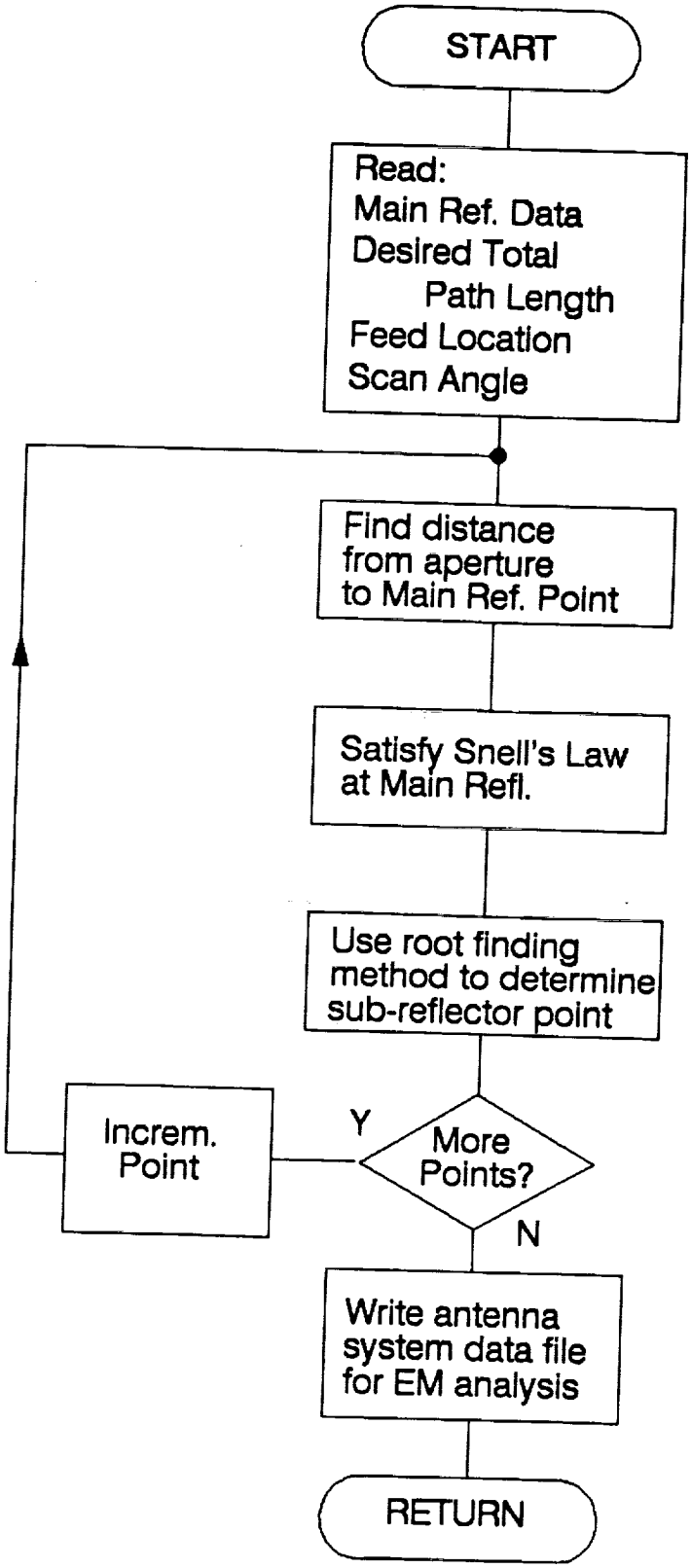

Figure 3.3-2 Two-dimensional dynamically reshaping sub-reflector generator subroutine RESHAP2D.FOR.

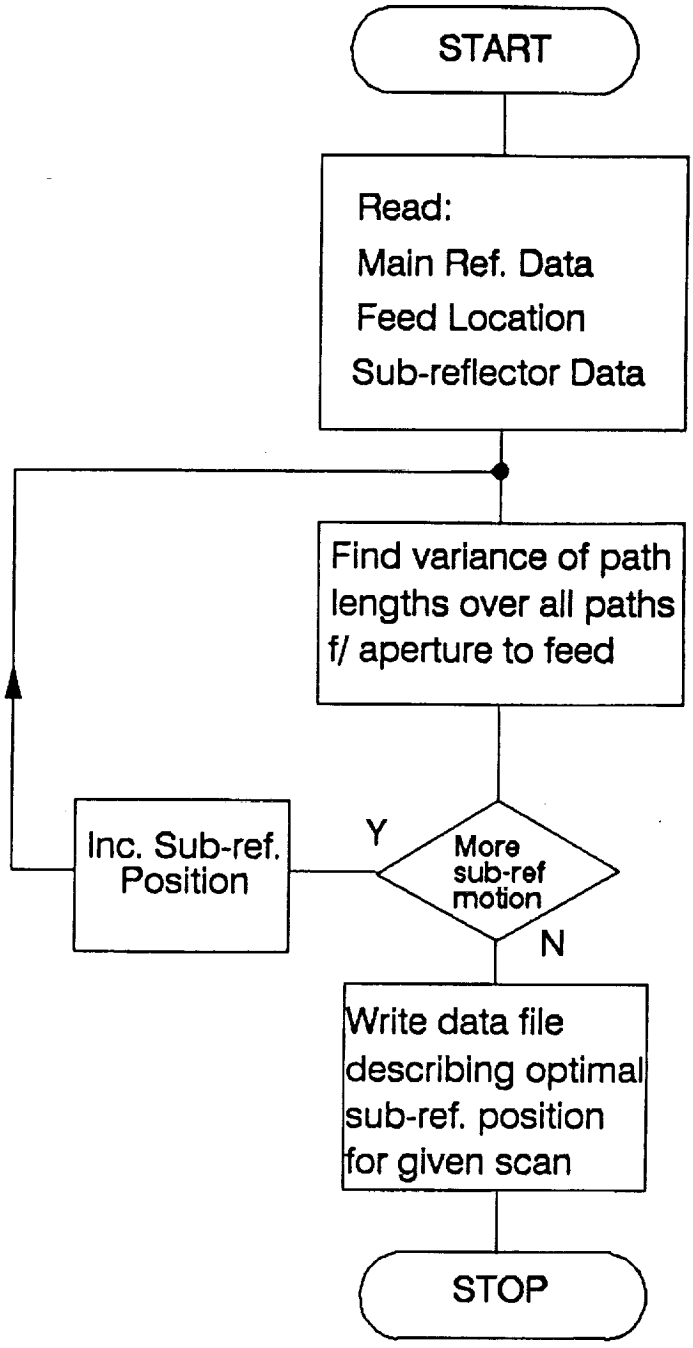

Figure 3.3-3 Two-dimensional statically shaped sub-reflector movement optimization sub-routine FITTER2D.FOR.

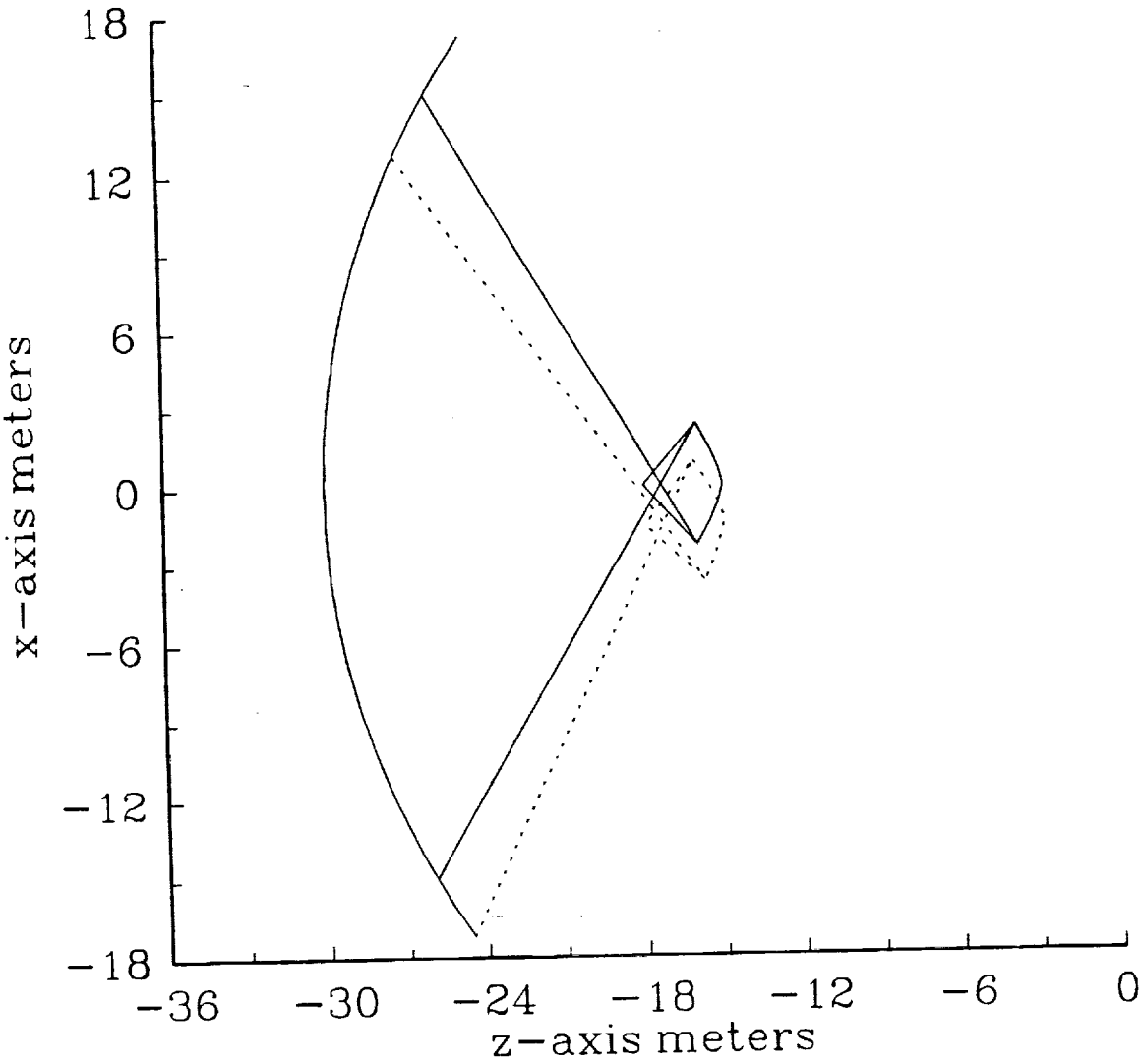

Figure 3.4-1. Scanning scenario for spherical reflector antenna with a correcting subreflector. The reflector system is configured to allow for ±5° of scan with no spillover (as defined by the edge rays), and to have a 30 m illuminated region of the 36m-main reflector. Solid lines represent edge rays for 0° scan direction. Dashed lines represent edge rays for +5° scan direction.

a unit during scan. The reflector system is designed to have an illuminated region over the main reflector of 30 m for all directions of scan. As is seen in Fig. 3.4-1, to accomplish this with no spillover over the ±5° of scan, the physical diameter of the main reflector must be 36 m. The ratio of the instantaneously illuminated portion of the main reflector for any direction of scan to the total diameter of the reflector is 30/36 = 0.833. This aperture use factor leads to a reduced aperture efficiency.

One possibility for increasing the aperture efficiency of the spherical reflector is to use an oversized correcting subreflector and allow relative motion between the feed and subreflector as shown in Fig. 3.4-2. In this case the main reflector has the same spherical curvature as the reflector shown in Fig. 3.4-1; however, a 30 m main reflector is sufficient to provide a 30 m illuminated region for all directions of scan. This greatly improves the aperture efficiency of the system at the expense of even more complicated feed motion.

The "extended aperture efficiency spherical reflector" is currently being evaluated at Virginia Tech. If this configuration proves to be successful, offset configurations will be included in the investigation. There is also the possibility of using two subreflectors to both correct for spherical aberration and reduce the crosspolarization inherent in offset reflector systems. If a large number of smaller subreflectors are used, there is also the possibility of reducing or even eliminating feed motion.

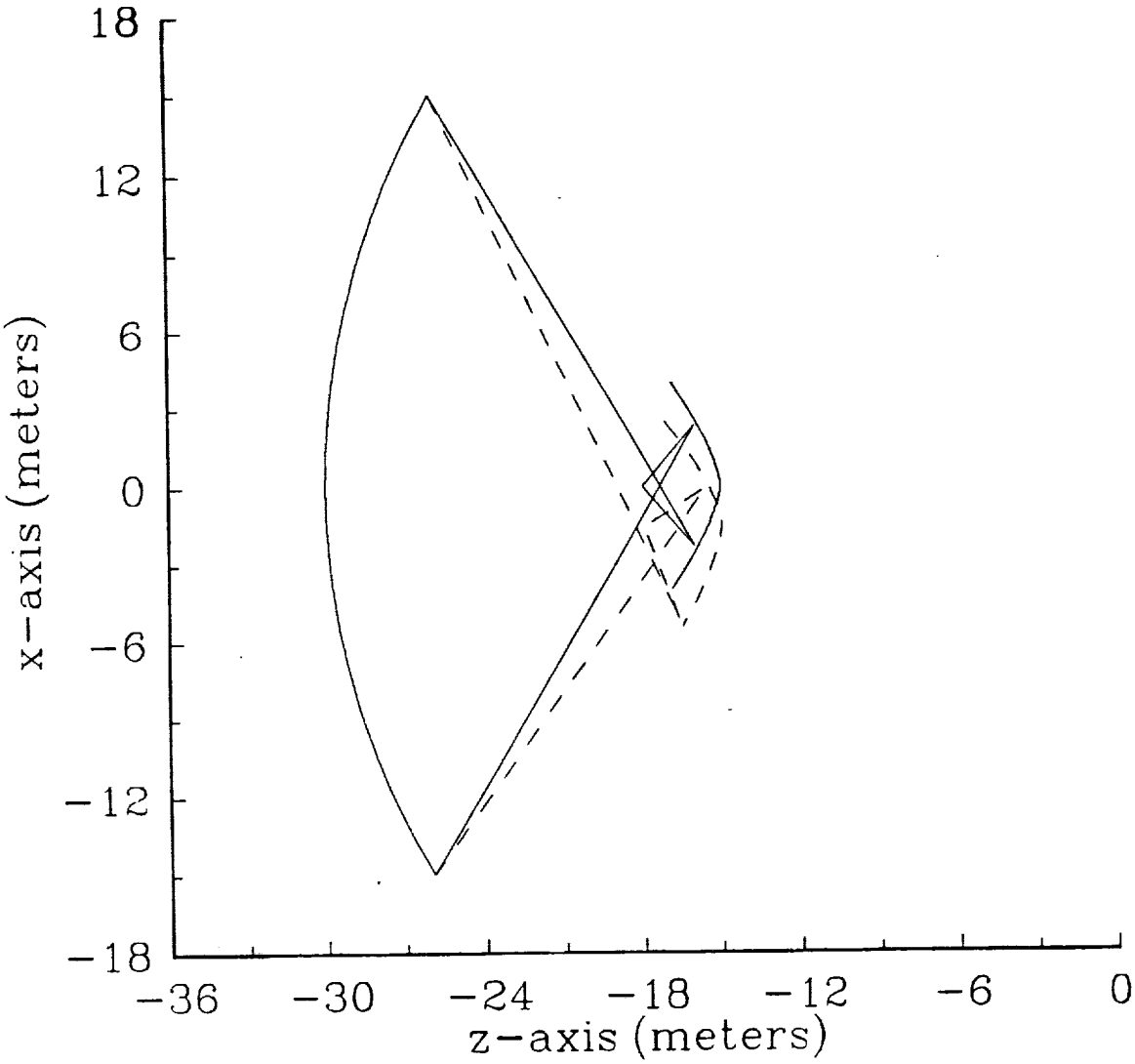

Figure 3.4-2. Scanning scenario for an "extended aperture efficiency spherical reflector antenna". An oversized subreflector and relative motion between the feed and subreflector allow for ±5° of scan with no spillover and no loss in aperture efficiency. Solid lines represents edge rays for 0° scan direction, perforated lines represents edge rays for +5° scan direction.

3.5 Multiple Reflector Imaging Systems

Array fed multiple reflector imaging systems are hybrid systems consisting of a large parabolic main reflector, one or more subreflectors in an imaging configuration, and a phased array. Using the reflectors in imaging arrangement a "magnified" image of the feed array is formed in the aperture of the main reflector. The radiation patterns may then be synthesized using ordinary array synthesis techniques. Analysis of secondary patterns of axisymmetric dual parabolic reflectors were reported in the Phase I final report.

To understand the scanning capabilities of imaging systems, focal plane region fields were analyzed. For the dual parabolic imaging system shown in Fig. 3.5-1, the main reflector is fed with a plane wave incident from angle θ_o, then fields in the plane of the feed array are calculated. The system has a 100 λ parabolic main reflector with a 100 λ focal length, and a 50 λ parabolic subreflector with a 50 λ focal length. The reflectors share a common focal point. Figures 3.5-2 a) and b) show the focal plane fields for the plane wave incidence from $\theta_o = 0°$ and $\theta_o = 5°$, respectively. The patterns were calculated using modified MRAPCA described in Section 2.2. Well behaved magnitude patterns and almost constant phase tilt in focal plane fields suggest, as expected, that for a moderately sized reflectors with a small magnification (M=2), the beam can be scanned by a simple linear phase tilt of the array element excitations. Analysis of imaging systems with larger main reflector diameters (D=25 m) and larger magnifications (M=3.5~4.5) are currently being conducted.

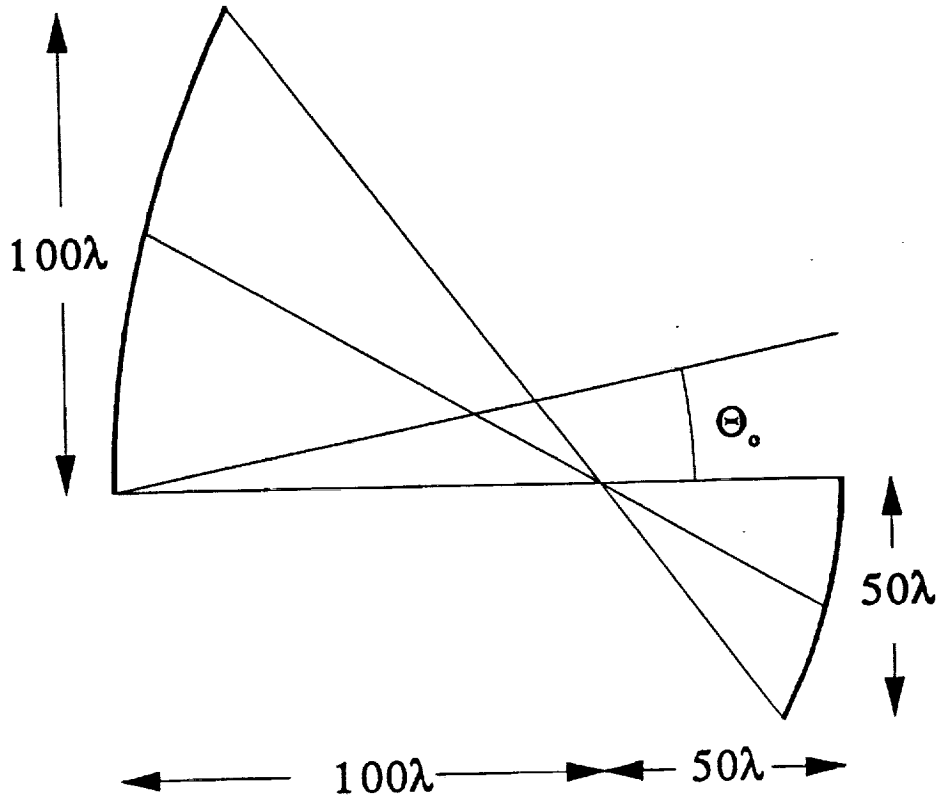

Figure 3.5-1. Geometry of a dual parabolic imaging reflector system.

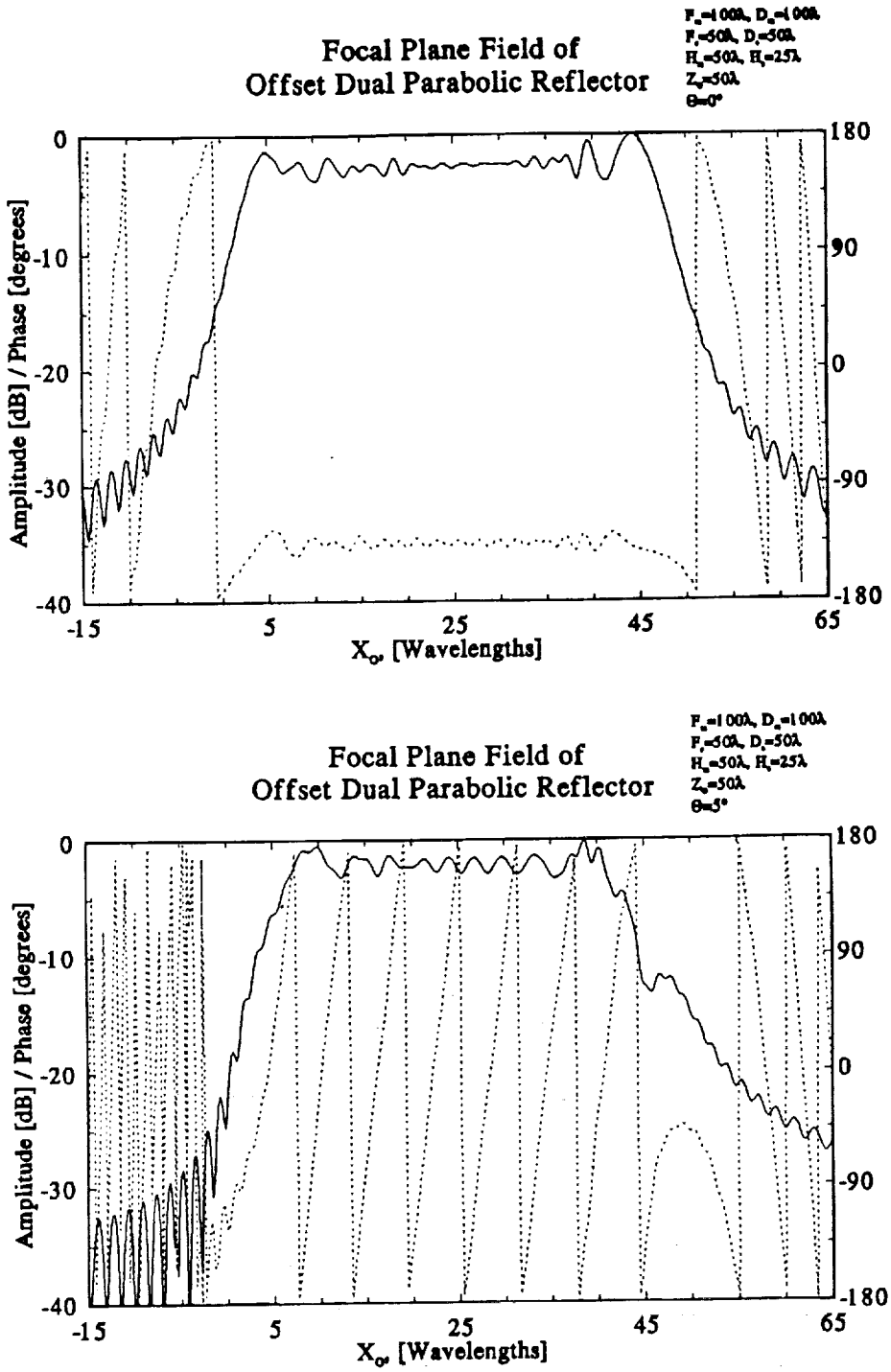

Figure 3.5-2. Focal plane region field of a dual parabolic reflector: a) θ_o=0°, b) θ_o=5°.

4. Radiometric array design

This project (item 3 in Table 1-1) is reported in detail in a separate semi-annual report. Here we only highlight the progress.

In the development of the reflector concepts it is taken for granted that a small feed array will be needed for beam steering and surface distortion correction. This work is aimed at developing array analysis and design techniques for radiometric applications. Our goal is to develop models that can be used to evaluate the noise performance of array and feed network architectures. Toward this end we have created a generalized analytical model to characterize the effects of noise contributions from each part of the array/feed system.

Our model considers the array and feed network as separate units, each of which can be characterized as an N-port network by its scattering parameters. The scattering parameters of the array characterize the element mismatch and interelement mutual coupling which is determined, in part, by the physical arrangement of the array. The feed network scattering parameters characterize the mismatch at each port of the network, the transfer function of the network and cross coupling between ports of the network.

Noise contributions are included in the model as noise voltage sources. The external noise environment impresses a received voltage on each element of the array. It is these noise voltages that are the desired quantity to be measured by the radiometer. Noise contributions due to the feed network are modeled as voltage sources at each port of the network. These sources include noise due to both active and passive devices within the feed network. Figure 4-1 illustrates conceptually our model for an array and associated feed network. Using this same approach, the effects of receiver noise contributions can also be included in the model.

From this conceptual model we have developed a network model based on the scattering parameters as described above. An example of the network model is shown in Figure 4-2. Mathematically the network can be described by three matrix equations, one each for the array elements, the feed network, and the receiver. Using these matrix equations we have developed an expression for the total received voltage at the receiver. This expression includes the effects of all noise sources in the system, the external noise environment, contributions from the feed network, and contributions from the receiver. From this expression for the received voltage, the total received power, the actual measured quantity in a radiometric system, can be found. To our knowledge, no one has examined noise effects in an array in such a generalized manner.

We are using the received noise power model we have developed to evaluate the relative merits of various feed network architectures. One design issue we are addressing is the use of active devices in the feed network, i.e. low noise amplifiers and electronically controlled phase shifters. We are now attempting to develop a figure of merit for comparing the various network designs.

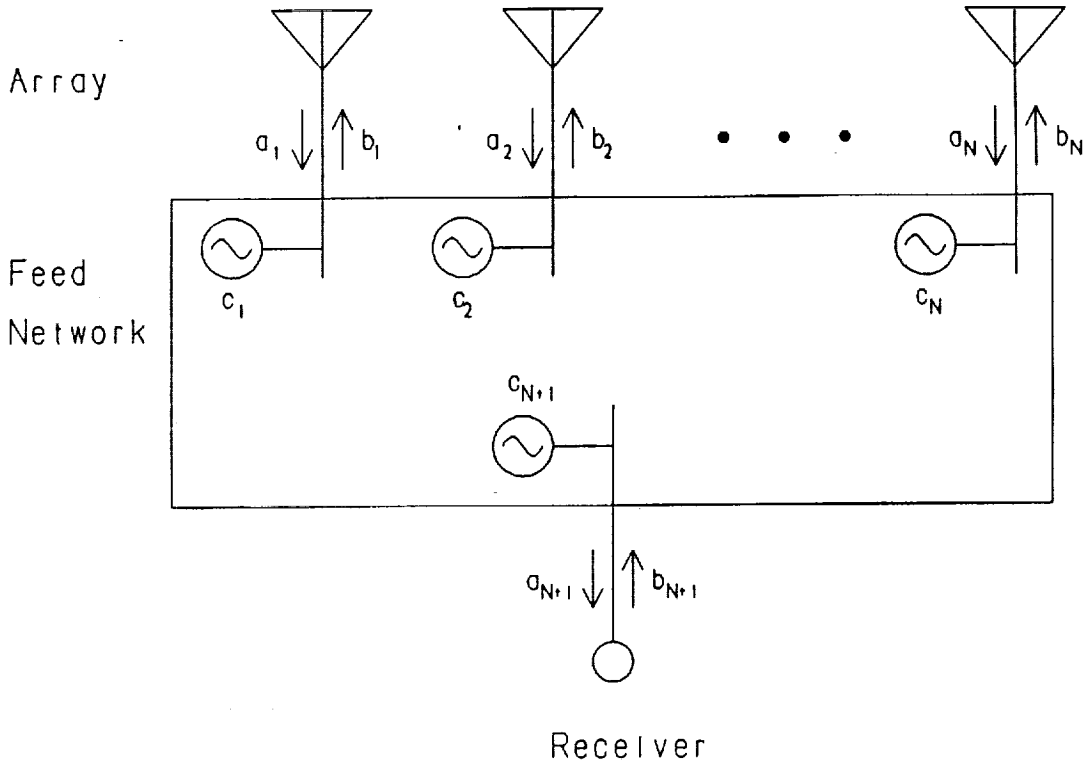

Figure 4-1. Model of array and feed network with noise sources.

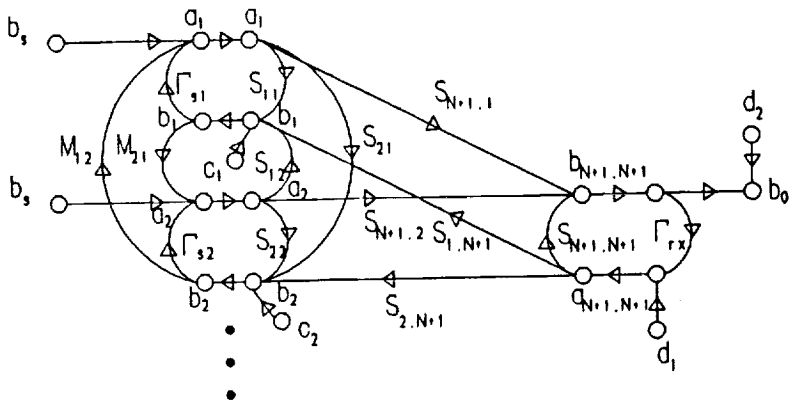

Figure 4-2. Generalized network model (signal flow graph) for an array and associated feed network.

semiannu.al
d:\wls
02/28/91

DISTRIBUTION

	Copies
NASA Scientific and Technical Information Facility P.O. Box 8757 Baltimore/Washington International Airport Maryland 21210	2
NASA Langley Aquisitions Division Attention: Richard Siebels Mail Stop 126 Langley Station Hampton, VA 23665-5225	Title page
Virginia Tech Office of Sponsored Programs Attention: Bonnie Beasley	Title page
NASA Langley Antennas and Microwave Research Branch Mail Stop 490 Langley Station Hampton, VA 23665	
Attention: Tom Campbell	1
Attention: M.C. Bailey	1
Attention: L.C. Schroeder	1